REACTOR THEORY AND POWER REACTORS

1. Calculational methods for reactors
2. Reactor kinetics

A.F. HENRY,
Massachusetts Institute of Technology,
Cambridge, MA,
United States of America

ABSTRACT

1 Calculational Methods for Reactors

1) The Few-Group Diffusion Equations

Write the few-group equations in continuous space form reviewing qualitatively the significance of the terms and the approximations made in deriving the few-group parameters. Discuss boundary and continuity conditions. Show a sketch of a BWR fuel assembly for which the few group equations must be solved.

2) The Finite Difference Method

Derive few-group finite difference equations first for a homongeneous, one-dimensional case and then for a heterogeneous, multidimensional case. Discuss the difference between mesh-centered and interface centered schemes. Indicate the magnitude of the problems of obtaining numerical solutions and sketch the elementary iteration methods used to overcome these problems. Quote without proof some of the basic tneorems used to guarantee convergence to a unique solution.

3) Advanced Methods for Cores with Explicitly Represented Heterogeneities

Practical limitations of the finite difference method. The synthesis approach - the basic idea and a derivation of the fundamental synthesis equations by the weighted residual method. Advantages and disadvantages of the synthesis approach.

The response matrix method - basic ideas, equations, virtues and limitations of the method.

4) Methods for Cores Represented by Large Homogenized Nodes

Qualitative review of the problem of determining equivalent homogeneous few group parameters for heterogeneous nodes (covered in more depth during the first week of course). The basic idea of nodal methods. Derivation of nodal equations from an assumed mathematical form for the group flux shapes throughout a node. Virtues and deficiencies of the nodal approach.

The finite element method: a variational principle yielding the group diffusion equations and derivations of the FEM from tnat principle. Advantages and disadvantages of the method.

5) Extension of the Above Methods to Depletion

(Fuel depletion equations assumed covered in 2.2.)

The tandom method: block depletion; flux renormalization; the use of fitted few group constants (if not covered in 2.2).

2. Reactor Kinetics

1) Space Dependent Kinetics Equations

Derivation of the time dependent few group diffusion equations and discussion of the problems of extending the methods described in (2.1) to transient cases. Finite difference treatment of the time part of the equation. Qualitative sketch of matrix splitting methods (alternating direction schemes). The quasi static method.

2) Point Kinetics

Derivation of the point kinetics equations. Definition and interpretation of the point kinetics parameters. Computation of the point kinetics parameters: use of the adjoint flux and the meaning of neutron importance. The perturbation expression for reactivity and approximate methods for computing reactivity based upon it. Measurements of reactivity: period and rod-drop techniques.

3) Feedback Phenomena

Derivation of simple heat transfer equations. Reactivity coefficients and their use along with the point kinetics and heat transfer equations in analysing reactor transients. Limitation of the point kinetics equations. The analysis of catastrophic accidents.

1 Calculational Methods for Reactors

Introduction

To determine the characteristics and behavior of a nuclear power reactor it is necessary to know the nuclear reaction rates throughout the reactor. These rates in turn depend on the local concentrations of materials and the local concentration of neutrons. Thus, if there are $n^j(\underline{r},t)$ *nucleii* of isotope-j per unit volume present at point $\underline{r}$ in the reactor at time t and if there are $N(\underline{r},E,t)dVdE$ neutrons having energies E in the range dE present in a small volume dV containing point $\underline{r}$, then the interaction rate for type α interactions (where α can stand for fission, or absorption or scattering, etc.) is given by

# of type-α interactions between neutrons and isotope-j per second in dVdE

$$= n^j(\underline{r},t)\sigma_\alpha{}^j(E)v(E)N(\underline{r},E,t)dVdE \tag{1.1}$$

where $\sigma_\alpha{}^j(E)$ is the microscopic cross section for interaction-α between neutrons of energy E and isotope-j, and v(E) is the neutron speed corresponding to kinetic energy E. (Recall that this relationship implies that an average over the thermal motions of the nuclei has been made. Thus $\sigma_\alpha{}^j(E)$ may depend on the temperature of the medium at point $\underline{r}$.)

If there are a mixture of isotopes within dV and we introduce the standard notations

$$\Sigma_\alpha(r,E,t) \equiv \sum_j n^j(\underline{r},t)\sigma_\alpha{}^j \equiv \text{microscope cross section for interaction } \alpha \text{ at point } \underline{r}, \text{ time } t \tag{1.2}$$

$$\phi(\underline{r},E,t) \equiv v(E)\,N(\underline{r},E,t) \equiv \text{scalar flux density} \tag{1.3}$$

we may sum Eq. 1.1 over all isotopes-j present within dV to obtain

# of type-α interactions per second in dVdE

$$= \Sigma_\alpha(\underline{r},E,t)\ \phi(\underline{r},E,t)\ dVdE \tag{1.4}$$

Integration of this result over all neutron energies gives the total number of type-α interactions per second within dV.

Since the material configuration of a reactor is either known (at beginning of life) or can be determined from past flux history and since we shall assume that needed microscopic cross sections are available, the principle problem of reactor physics is to determine the scalar flux density $\phi(\underline{r},E,t)$.

The present section deals with the few group diffusion theory approximation for determining $\phi(\underline{r},E)$. (Although the methods we shall discuss can all be extended to the time dependent case, we shall here be concerned only with static solutions.) In what follows we shall sketch the derivation of the few group diffusion equations emphasizing the physical assumptions involved. Then we shall discuss solution methods - finite difference, synthesis, response matrix, finite element and nodal schemes. Finally, some of the mechanical problems of extending the procedures to depletion will be discussed.

1.1 The Few-Group Diffusion Equations

a) Reaction Rates

To derive the few group diffusion approximation we shall start with an exact relationship expressing mathematically the physical statement that for a critical reactor in a stationary condition the rate at which neutrons having energies in the range dE appear within dV equals the rate at which they disappear.

Neutrons may appear in dEdV because of scattering from other energies or as the result of fissions taking place within dV. To describe the first of these processes we make use of the macroscopic differential scattering cross section $\Sigma_s(\underline{r},E'\to E)dE$ for neutrons at $\underline{r}$ scattering from energy E' to some energy E in the interval dE. In terms of this cross section (and in analogy with (1.4) we have

(# of neutrons/sec scattering from dE' into dE within dV)

$$= \Sigma_s(\underline{r},E'\to E)\phi(\underline{r},E')dE'dEdV \qquad (1.5)$$

Integration of this expression over all initial energies E' gives the total rate at which neutrons appear in dEdV because of scattering.

The rate at which neutrons appear in dVdE because of fission in dVdE equals the number of fissions in dVdE' per second $\Sigma_f(\underline{r},E')\ \phi(\underline{r},E')\ dE'dV$ multiplied by ν, the average number of neutrons emitted per fission, and by $\chi(E)dE$, the fraction of fission neutrons emitted in the energy interval dE. Thus we have,

(# of neutrons/sec appearing in dVdE because of fission)

$$= \chi(E)dE\ \left(\int_0^\infty \nu\Sigma_f(\underline{r},E')\phi(\underline{r},E')dE'\right)dV \qquad (1.6)$$

(To simplify notation we neglect the fact that the "fission spectrum" is different for different fissionable isotopes, U^{235}, Pu^{239}, U^{238}, etc.)

The rate at which neutrons disappear from dEdV equals the rate at which they interact (scatter to different energies or undergo absorption) plus the net rate at which those in dE leak out of dV. The first rate is given by

(total number of interactions in dVdE per second) $= \Sigma_t(\underline{r},E)\phi(\underline{r},E)dVdE \qquad (1.7)$

where $\Sigma_t(\underline{r},E)$ is the total macroscopic interaction cross section (scattering, (nγ), fission - any process that removes a neutron from dE).

b) The Net Current Density

To derive an expression for the net rate at which neutrons leak out of dV we introduce the net current density $\underline{J}(\underline{r},E)$. This quantity is defined physically by noting that for any small surface element dS containing point $\underline{r}$ and oriented such that the unit vector $\underline{n}$ is normal to the surface there are a net number of neutrons per second passing through dS (the difference

between those crossing at any angle from the rear to the front of dS and those crossing at any angle from front to rear). The magnitude of this net flow rate will depend on the orientation of dS (i.e. the direction of the normal $\underline{n}$). Moreover, for one orientation of dS (one direction of $\underline{n}$) the net flow will be a maximum. With this physical picture in mind we define the net current density $\underline{J}(\underline{r},E)$ as follows:

> $\underline{J}(\underline{r},E)dEdS$ is the net number of neutrons per second having energies in dE and passing through dS when the orientation of dS is such that net number is a maximum. The direction of $\underline{J}(\underline{r},E)$ is the direction of the normal to dS when that orientation is such that the magnitude $|\underline{J}(\underline{r},E)|$ is a maximum.

When the orientation ($\underline{n}$) of dS is not such that the net flow is a maximum (i.e. when $\underline{n} \neq \frac{\underline{J}(\underline{r},E)}{|\underline{J}(\underline{r},E)|}$) it can be shown that the net flow through dS is given by the projection of $\underline{J}$ on $\underline{n}$. Thus we have:

$$\begin{pmatrix}\text{Net number of neutrons with energies in dE passing per second through a surface dS having normal } \underline{n}\end{pmatrix} = \underline{n} \cdot \underline{J}(\underline{r},E)dEdS \qquad (1.8)$$

It should be noted that, although $\underline{J}(\underline{r},E)$ is essentially positive, $\underline{n} \cdot \underline{J}$ can be negative. Physically this situation implies that dS is so oriented that the number of neutrons crossing per second from the (+) to the (-) side of dS exceeds the number flowing from the (-) to the (+) side. (See Fig. 1.)

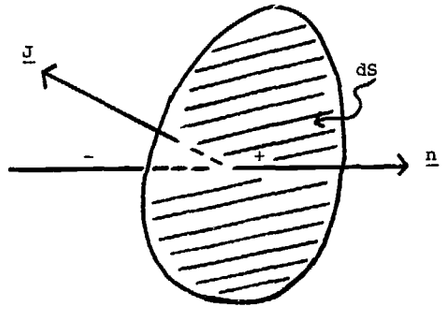

Fig. 1: Net Current Through A Surface Element

Equation (1.8) permits us to obtain an expression for the rate of leakage of neutrons from a volume V having a surface S. If dS is an element of S and $\underline{n}$ its outward directed normal, we have

$$\begin{pmatrix}\text{net \# of neutrons with energy E in dE leaking out of V per second}\end{pmatrix} = \left[\int_S \underline{n} \cdot \underline{J}(\underline{r},E)\, dS\right] dE \qquad (1.9)$$

But, by Gauss's Law,

$$\int_S \underline{n} \cdot \underline{J}\, dS = \int_V \nabla \cdot \underline{J}\, dV$$

Thus, if V is very small (of size dV) we have

$$\begin{pmatrix}\text{net \# of neutrons Having energies within dE leaking out of dV per second}\end{pmatrix} = \nabla \cdot \underline{J}(\underline{r},E)\, dVdE \qquad (1.10)$$

If $\nabla \cdot J$ dVdE is negative there are more neutrons in dE leaking into dV than there are leaking out.

c) The Balance Condition

We now have all the terms needed to express mathematically the criticality condition.

For a critical reactor in a steady state operating condition the rate at which neutrons appear in any "volume of phase space" dVdE exactly equals the rate at which they disappear. Combining 1.5 (integrated over E') 1.6, 1.6 and 1.10, we get the fundamental equation

$$\nabla \cdot \underline{J}(\underline{r},E) + \Sigma_t(\underline{r},E)\phi(\underline{r},E) = \int_0^\infty dE' \left[\Sigma_s(\underline{r},E'\to E) + \chi(E)\nu\Sigma_f(\underline{r},E')\right] \phi(\underline{r},E') \qquad (1.11)$$

d) The P-1 Approximation

Insofar as statistical fluctuations in the neutron population may be neglected, this equation is exact. However, since it involves both $\underline{J}$ and ϕ, it is not complete. We need another relationship between $\underline{J}$ and ϕ before either one can be solved for. To obtain this second relationship we shall make what is called the "P-1 Approximation to the Transport Equation". This approximation states that the "directional flux density" $v(E)N(\underline{r},\underline{\Omega},E)$ (where $N(\underline{r},\underline{\Omega},E)$ dVdΩdE is the number of neutrons in dV with energies in dE and all travelling with directions $\underline{\Omega}$ within the cone of directions dΩ) can be approximated by

$$N(\underline{r},\underline{\Omega},E) \simeq F(\underline{r},E) + \underline{\Omega} \cdot \underline{V}(\underline{r},E) \qquad (1.12)$$

where $F(\underline{r},E)$ is a scalar function and $\underline{V}(\underline{r},E)$ is a vector function. ($\underline{\Omega} \cdot \underline{V}(\underline{r},E) = \Omega_x V_x(\underline{r},E) + \Omega_y V_y(\underline{r},E) + \Omega_z V_z(\underline{r},E)$, Ω_x, Ω_y and Ω_z being the components of the unit vector $\underline{\Omega}$ in the coordinate directions X, Y and Z.)

Physically, Eq. 1.12 states that the angular distribution of neutrons in dVdE is linear in the direction cosines Ω_x, Ω_y and Ω_z. Thus 1.12) will never be a good representation of a beam of neutrons. The P-1 approximation will be valid only when the angular distribution of $N(r,\Omega,E)$ is almost isotropic.

The physical definitions of $\phi(\underline{r},E)$ and $\underline{J}(\underline{r},E)$ can be shown to imply mathematically that

$$\phi(\underline{r},E) = \int_\Omega v(E)\, N(\underline{r},\underline{\Omega},E)\, d\Omega \qquad (1.13)$$

and

$$\underline{J}(\underline{r},E) = \int_\Omega \underline{\Omega}\, v(E) N(\underline{r},\underline{\Omega},E)\, d\Omega \qquad (1.14)$$

Substitution of (1.12) into these relationships in turn implies that (1.12) can be written

$$v(E)N(\underline{r},\underline{\Omega},E) \simeq \phi(\underline{r},E) + 3\underline{\Omega} \cdot \underline{J}(\underline{r},E) \qquad (1.15)$$

If we substitute this result into the basic equation for $N(\underline{r},\underline{\Omega},E)$ (the neutron transport equation) and require the result to be valid when integrated overall $\underline{\Omega}$ we obtain (1.11). If in addition we substitute (1.15) into the transport equation, multiply by $\underline{\Omega}$ and then require the result to be valid when integrated overall Ω we obtain "the second P-1 equation"

$$\nabla\phi(\underline{r},E) + 3\Sigma_t(\underline{r},E)\,\underline{J}(\underline{r},E) = \int_o^\infty \Sigma_{s_1}(\underline{r},E'\to E)\underline{J}(\underline{r},E')dE' \qquad (1.16)$$

where

$$\Sigma_{s_1}(\underline{r},E'\to E) = \int_{-1}^{+1} \tfrac{1}{2}\cos\theta\ \Sigma_s(\underline{r},E'\to E,\ \cos\theta)\ d(\cos\theta)$$

This is a vector equation relating the three components of $\underline{J}$ to the gradient of ϕ. It is approximate since it is based on the approximation (1.15). We shall use 1.11 and 1.16 to derive the few group diffusion theory approximation.

e) The Few Group Approximation

The basis of the few group approximation is the fact that several mean free paths inside a homogeneous medium the space and energy parts of $\phi(\underline{r},E)$ and $\underline{J}(\underline{r},E)$ become separable so that these quantities may be written

$$\phi(\underline{r},E) = \phi(\underline{r})\ F_o^j(E)$$

$$\underline{J}(\underline{r},E) = \underline{J}(\underline{r})\ F_1^j(E) \qquad (1.17)$$

$\underline{r}$ far inside homogeneous region j.

where the "spectrum functions" $F_o^j(E)$ and $F_1^j(E)$ are characteristic of medium-j. They may be found by substituting (1.17) into (1.11) and (1.16) and making the assumption that $\phi(\underline{r}) \sim \underline{J}(\underline{r}) \sim e^{i\underline{B}\cdot\underline{r}}$, B^2 being the "materials buckling" of the homogeneous material.

Thus, if j and j+1 label two adjacent homogeneous regions, the scalar flux density $\phi(\underline{r},E)$ is $\phi(\underline{r})F_o^j(E)$ well within region j and $\phi(\underline{r})F_o^{j+1}(E)$ well within region (j+1). However, these separable expressions for $\phi(\underline{r},E)$ cannot be physically valid at the interface between regions-j and (j+1) since $F_o^j(E) \neq F_o^{j+1}(E)$, and thus the approximate representation of $\phi(\underline{r},E)$ must there be discontinuous at almost all energies - an unphysical condition. We thus face the dilemna of wanting to use (1.17) since it is known to be correct throughout most of region j but not being able to, since it violates the continuity of flux and current conditions on the interfaces between j and its neighboring regions. In few group theory this dilemna is resolved by abandoning the requirement that flux and current be continuous at all energies and replacing it with the weaker requirement that these conditions be obeyed in an integral sense over each of certain energy intervals ΔE_g into which we split the energy range 0 → 15 MeV (the range of interest for fission reactors). Thus for a G-group theory, rather than require that $\phi(r,E)$ and the normal component $\underline{n}\cdot\underline{J}(\underline{r},E)$ be continuous across an interface at all energies we require merely that $\int_{\Delta E_g}\phi(\underline{r},E)dE$ and $\int_{\Delta E_g}\underline{n}\cdot\underline{J}(\underline{r},E)dE$ (g = 1, 2 ... G) be continuous.

To construct expressions for $\phi(\underline{r},E)$ and $\underline{J}(\underline{r},E)$ that meet these integral conditions and yet obey (1.17) far inside region j we renormalize pieces of $F_o^j(E)$ and $F_1^j(E)$ by defining

$$F_{og}^j(E) \equiv \frac{1}{\int_{\Delta E_g} F_o^j(E)} F_o^j(E) \tag{1.18}$$

$$F_{1g}^j(E) \equiv \frac{1}{\int_{\Delta E_g} F_1^j(E)} F_1^j(E)$$

$g = 1, 2, \ldots G;\ j = 1, 2, \ldots J$

so that

$$\int_{\Delta E_g} F_{og}^j(E)\,dE = \int_{\Delta E_g} F_{1g}^j(E)\,dE = 1 \tag{1.19}$$

Then we approximate the flux and net current densities throughout region j as

$$\phi(\underline{r},E) \simeq \phi_g(r)\ F_{og}^j(E)$$

$$\underline{J}(\underline{r},E) \simeq \underline{J}_g(\underline{r})\ F_{1g}^j(E) \qquad E \subset \Delta E_g;\ \underline{r} \subset \text{region } j \qquad g = 1, 2, \ldots G \tag{1.20}$$

In view of Eq. (1.19) we then have (with S^+ and S^- referring to the (+) and (-) sides of the interface between j and (j+1))

$$\int_{\Delta E_g} dE\ \phi(\underline{r},E)\big|_{S^-} = \phi_g(\underline{r})\big|_{S^-} = \int_{\Delta E_g} dE\ \phi(\underline{r},E)\big|_{S^+} = \phi_g(r)\big|_{S^+}$$

$$\int_{\Delta E_g} dE\ \underline{n}\cdot\underline{J}(\underline{r},E)\big|_{S^-} = \underline{n}\cdot\underline{J}_g(\underline{r})\big|_{S^-} = \int_{\Delta E_g} dE\ \underline{n}\cdot\underline{J}(\underline{r},E)\big|_{S^+}$$

$$= \underline{n}\cdot\underline{J}_g(\underline{r})\big|_{S^+} \tag{1.21}$$

In words: the flux and normal component of the net current will be continuous in an integral sense provided $\phi_g(\underline{r})$ and $\underline{n}\cdot J_g(\underline{r})$ are required to be continuous.

Moreover, it can be shown that for inside each homogeneous region-j

$$\frac{\phi_1(\underline{r})}{\int_{\Delta E_1} F_o^j(E)dE} = \frac{\phi_2(\underline{r})}{\int_{\Delta E_2} F_o^j(E)dE} = \ldots = \frac{\phi_G(\underline{r})}{\int_{\Delta E_G} F_o^j(E)dE} \tag{1.22}$$

$$\frac{\underline{J}_1(\underline{r})}{\int_{\Delta E_1} F_1^j(E)dE} = \frac{\underline{J}_2(\underline{r})}{\int_{\Delta E_2} F_1^j(E)dE} = \ldots = \frac{\underline{J}_G(\underline{r})}{\int_{\Delta E_G} F_1^j(E)dE}$$

Eq. (1.18) then shows that, as desired, the group expressions (1.20) reduce to the completely separable expressions (1.17).

These considerations suggest that the few group equations we shall derive should describe quite accurately a reactor composed of large homogeneous regions.

Unfortunately, most reactors are not so constructed. At best they contain uniform lattices of fuel rods, cladding and associated coolant and moderator. For the fuel element "cells" making up such lattices neither the basic assumption (1.12) of the P-1 approximation nor the asymptotic separability assumption

(1.17) are valid. For these situations it is necessary to find "equivalent homogenized" group-parameters. Such matters were discussed during the first week of this course. We shall not repeat that material but rather shall continue the derivation of the few group diffusion equations assuming the reactor regions to be homogeneous. It is important to note, however, that the simple expressions we shall obtain for the few group parameters must be modified to account for lattice effects when real reactors are being analysed.

f) The Few Group Diffusion Equations

To obtain the few group diffusion equations we first substitute (1.20) into (1.11) and (1.16) and require the result to be true when integrated over each of the ΔE_g's. When (1.19) is applied, the result for (1.11) is

$$\nabla\cdot\underline{J}_g(\underline{r}) + \int_{\Delta E_g}\Sigma_t(\underline{r},E)F^j_{og}(E)dE \quad \phi_g(\underline{r}) =$$

$$= \sum_{j'=1}^{G}\int_{\Delta E_g}dE\int_{\Delta E_{g'}}dE'\Sigma_s(\underline{r},E'\to E)F^j_{og'}(E')\ \phi_{g'}(\underline{r}) + \qquad (1.23)$$

$$= \sum_{g'}\int_{\Delta E_g}dE\chi(E)\int_{\Delta E_{g'}}dE\ \nu\Sigma_f(\underline{r},E')F^j_{og'}(E')\ \phi_{g'}(\underline{r})$$

where the appropriate value of j (and hence $F^j_{og}(E)$) will change depending on the location of point $\underline{r}$.

To simplify notation we rewrite (1.23) as

$$\nabla\cdot\underline{J}_g(\underline{r}) + \Sigma_{f_g}(\underline{r})\ \phi_g(r) =$$

$$= \sum_{j'=1}^{G}\left[\Sigma_{gg'}(\underline{r}) + \chi_g\nu\Sigma_{fg'}(\underline{r})\right]\phi_{g'}(\underline{r}) \qquad (1.24)$$

where the total group-g interaction cross section ($\Sigma_{t_g}(\underline{r})$), the transfer cross section from group-g' to group-g ($\Sigma_{gg'}(\underline{r})$, the fission spectrum for group-g (χ_g) and the neutron production cross section due to fission in group-g' ($\nu\Sigma_{f_{g'}}(\underline{r})$ are defined by comparison with (1.23).

If we were to carry out an analogous procedure for the P-1 equation (1.16) (i.e. substitute (1.20) into (1.16) and require the result to be valid when integrated over ΔE_g) we would obtain a P-1 transfer term from group-g' to group-g completely analogous to the $\Sigma_{gg'}$, $\phi_{g'}$ terms of Eq. (1.24). As a result, the diffusion equation eventually obtained would involve Laplacian terms and diffusion coefficients transferring neutrons from one group to another. To avoid this complexity we make an additional approximation in reducing the right hand side of (1.16) to group form. Namely, rather than represent $\underline{J}(r,E')$ on the right hand side by the second of Eq. (1.20) we approximate it by the completely separable form (1.17).

Thus substituting (1.20) for $\phi(\underline{r},E)$ and $\underline{J}(\underline{r},E)$ on the left hand side and the 2^d of Eq. (1.17) for $\underline{J}(\underline{r},E')$ on the right hand side and integrating over ΔE_g, we get

$$\nabla\phi_g(\underline{r}) + 3\left(\int_{\Delta E_g}\Sigma_t(\underline{r},E)F_{1g}^j(E)dE\right)\underline{J}_g(\underline{r}) =$$

$$\int_{\Delta E_g}dE\int_o^\infty dE'\Sigma_s(\underline{r}\cdot E'\to E)\ F_1^j(E)\ \underline{J}(\underline{r}) =$$

$$\frac{\int_{\Delta E_g}dE\int_o^\infty dE'\Sigma_{s1}(r,E'\to E)\ F_1^j(E')\ \underline{J}_g(\underline{r})}{\int_{\Delta E_g}F_1^j(E)} \qquad (1.25)$$

where the last step comes from equating the expressions for $\int_{\Delta E_g}\underline{J}(\underline{r},E)dE$ obtained from (1.12) and (1.20).

If we define the "transport cross section" for group-g as

$$\Sigma_{tr\ g}(\underline{r}) \equiv \int_{\Delta E_g}\Sigma_t(\underline{r},E)F_{1g}^j(E)dE - \frac{\int_{\Delta E_g}dE\int_o^\infty dE'\Sigma_{s_1}(\underline{r},E'\to E)F_1^j(E')}{\int_{\Delta E_g}dE\ F_1^j(E)}$$

and the "diffusion constant" for group-g as

$$D_g(\underline{r}) \equiv \frac{1}{3\Sigma_{tr\ g}(r)} \qquad (1.26)$$

We obtain Fick's Law for group-g neutrons:

$$\underline{J}_g(\underline{r}) = -D_g(\underline{r})\nabla\phi_g(\underline{r}) \qquad (1.27)$$

Finally, substitution of this result into (1.24) gives us the few group diffusion equations

$$-\nabla\cdot D_g(\underline{r})\nabla\phi_g(\underline{r}) + \Sigma_{tg}(\underline{r})\phi_g(\underline{r}) =$$

$$= \sum_{g'=1}^{G}\left[\Sigma_{gg'}(\underline{r}) + \chi_g\nu\Sigma_{fg}(\underline{r})\right]\ \phi_{g'}(\underline{r}) \qquad (1.28)$$

$$g = 1,\ 2,\ \ldots\ G$$

In view of (1.21) and (1.27) we require that the $\phi_g(\underline{r})$ and the normal components $\underline{n}\cdot D_g(\underline{r})\nabla\phi_g(\underline{r})$ be continuous across internal surfaces. On the outer surface we shall require that the $\phi_g(\underline{r})$ vanish. Alternative boundary conditions that $\frac{1}{\phi_g(r)}\ \frac{\partial\phi_g(\underline{r})}{\partial n} = -2D_g(\underline{r})$ or that $\phi_g(\underline{r})$ vanish at a distance $2D_g(\underline{r})$ $\left(=\frac{2}{3\Sigma_{tr\ g}} = \frac{2}{3}\lambda_{tr\ g}\right)$ are somewhat more physical in that they are based on requiring that the integral over all incoming directions of the P-1 expression for the directional flux (1.15) vanish. However, the zero-flux boundary condition is simpler, and, when applied at the outer boundary of a reflector, all three boundary conditions lead to indistinguishable results.

We note again that, for lattices, finding the group parameters is far more complicated than the simple procedure we have sketched for a reactor composed of homogeneous regions. But the methods discussed in the first week of the course show that equivalent homogenized parameters can be found. It is also possible to find equivalent constants for control rod material or lumps of burnable poison. We shall not pursue the point other than to

note that meaningful few group diffusion theory parameters can be found for the fuel assembly shown in Figure 2 (containing three zones of enrichment; the box shown is one of a cluster of four surrounding a cross shaped control rod).

1.2 The Finite Difference Method

The solution of the group-diffusion equations by analytical methods is practical only for essentially one-dimensional situations involving only a few homogeneous regions within which the group

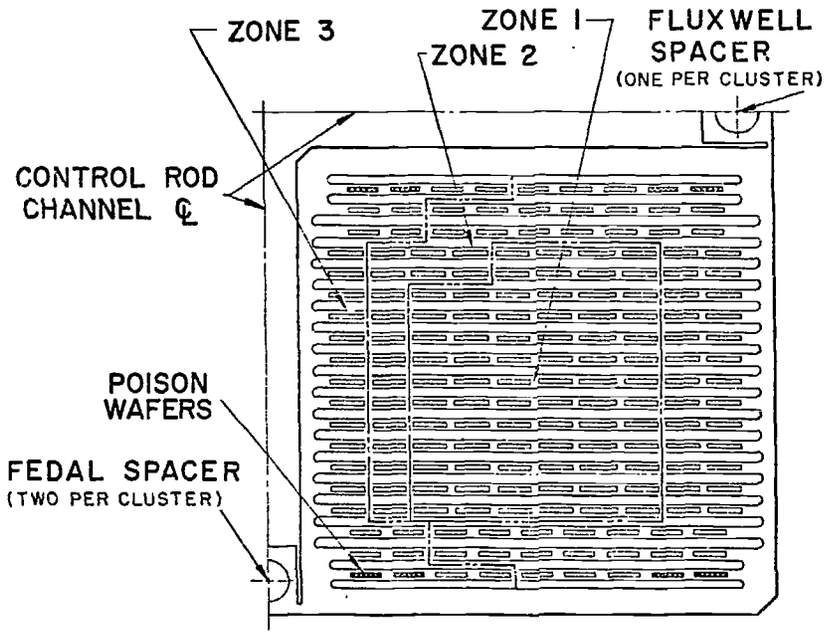

Figure 2. Fuel Subassembly

diffusion parameters are spatially constant. For mathematical models of a reactor that are more realistic numerical schemes must be used. The most common of these is the finite difference method. We shall examine two forms of this method for the one dimensional slab geometry case and then sketch generalizations to more dimensions.

a) The One-Dimensional Interface Centered Scheme

If for a Cartesian (XYZ) coordinate system the group parameters depend only on X and the reactor extends from $(-Z_1)$ to $(+Z_1)$ in the Z-direction and from $(-Y_1)$ to $(+Y_1)$ in the Y-direction, the solution for the $\phi_g(\underline{r})$ is separable and may be written

$$\phi_g(\underline{r}) = X_g(x) \cos \frac{\pi y}{2Y} \cos \frac{\pi z}{2Z} \tag{1.29}$$

a solution that meets the continuity conditions in the Y and Z-directions and vanishes at $y = \pm Y$; $z = \pm Z$. Substitution of (1.29) into (1.28) yields

$$- \frac{d}{dx} D_g(x) \frac{d}{dx} X_g(x) + \left[D_g(x) B_{yz}^2 + \Sigma_{tg}(x) \right] X_g(x) =$$

$$= \sum_{g'=1}^{G} \left[\Sigma_{gg'}(x) + \chi_g \nu \Sigma_{fg'}(x) \right] X_{g'}(x); \quad g = 1, 2, \ldots 3 \tag{1.30}$$

where B_{yz}^2 is the "transverse buckling".

$$B_{yz}^2 \equiv \left(\frac{\pi}{2Y_1}\right)^2 + \left(\frac{\pi}{2Z_1}\right)^2 \tag{1.31}$$

Equations (1.30) are the one-dimensional group-diffusion equations we wish to solve by the finite difference method. To do so we partition the X-dimension of the reactor as indicated in Fig. 3.

Next we integrate Eqs. (1.30) from $(x_n - \frac{h_{n-1}}{2})$ to $(x_n + \frac{h_n}{2})$ for n = 2, 3 ... N-1. The result is

$$D_g(x)\frac{d}{dx}X_g(x)\Big|_{x_n-\frac{h_{n-1}}{2}} - D_g(x)\frac{d}{dx}X_g(x)\Big|_{x_n+\frac{h_n}{2}} +$$

$$+\int_{x_n-\frac{h_{n-1}}{2}}^{x_n+\frac{h_n}{2}}\left[D_g(x)B_{yz}^2+\Sigma_{tg}(x)\right]X_g(x)dx =$$

$$=\sum_{g'=1}^{G}\int_{x_n-\frac{h_{n-1}}{2}}^{x_n-\frac{h_n}{2}}\left[\Sigma_{gg'}(x)+\chi_g\nu\Sigma_{fg'}(x)\right]X_g(x)dx$$

$$g = 1, 2, \ldots G;\ n = 2, 3, \ldots N-1 \qquad (1.32)$$

Finally, we approximate the group parameters within the intervals h_n by their average values (designated $D_g^{(n)}$, $\Sigma_{tg}^{(n)}$, etc.); we approximate the flux $X_g(x)$ in the interval $(x_n - \frac{h_{n-1}}{2}) \to (x_n + \frac{h_n}{2})$ by $X_g^{(n)} \equiv X_g(x_n)$, and we approximate the derivatives $\frac{d}{dx}X_g(x)\big|_{x_n+\frac{h_n}{2}}$ by

$$\frac{d}{dx}X_g(x)\Big|_{x_n+\frac{h_n}{2}} \simeq \frac{1}{h_n}\left[X_g^{(n+1)} - X_g^{(n)}\right] \qquad (1.33)$$

With these approximations Eqs. (1.32) becomes

$$D_g^{(n-1)}\frac{X_g^{(n)}-X_g^{(n-1)}}{h_{n-1}} - D_g^{(n)}\frac{X_g^{(n+1)}-X_g^{(n)}}{h_n} +$$

$$\tfrac{1}{2}\left[h_{n-1}(D_g^{(n-1)}B_{yz}^2+\Sigma_{tg}^{(n-1)})+h_n(D_g^{(n)}B_{yz}^2+\Sigma_{tg}^{(n)})\right]X_g^{(n)} =$$

$$\tfrac{1}{2}\sum_{g'=1}^{G}\left[h_{n-1}(\Sigma_{gg'}^{(n-1)}+\chi_g\nu\Sigma_{fg'}^{(n-1)})+(h_n(\Sigma_{gg'}^{(n)}+\chi_g\nu\Sigma_{fg'}^{(n)})\right]$$

$$g = 1, 2, \ldots G;\ n = 2, 3, \ldots N-1 \qquad (1.34)$$

These are the interface-centered, finite-difference, group-diffusion equations. With $X_g^{(0)} = X_g^{(N)} = 0$, there are exactly G(N-2) equations in G(N-2) unknowns. If, on the other hand, there is a symmetry boundary condition - for example at $x = x_N$ - then $X_g^{(N)} \neq 0$ and we extend (1.34) to n = N using the symmetry condition $X_g^{(N+1)} = X_g^{(N-1)}$ for the final equation.

b) Mesh Centered Difference Equations

To obtain mesh centered difference equations for (1.30) we again partition the X-domain as in Fig. 3 and approximate

the group parameters within the intervals h_n by their average values. However, in this case we integrate Eqs. (1.30) over intervals $x_n \to x_n + h_n$. With notation that accounts for possible discontinuities in the D_g and the $\frac{dX_g}{dx}$ at point $x = x_n$ we obtain

$$D_g^n \left[\frac{d}{dx} X_g(x) \Big|_{x_n^+} - \frac{d}{dx} X_g(x) \Big|_{x_{n+1}^-} \right] +$$

$$h_n (D_g^{(n)} B_{yz}^2 + \Sigma_{tg}^{(n)}) \bar{X}_g^{(n)} = \sum_{g'=1}^{G} h_n (\Sigma_{gg'}^{(n)} + \chi_g \nu \Sigma_{fg'}^{(n)}) \bar{X}_{g'}^{(n)} \qquad (1.35)$$

$$g = 1, 2 \ldots G; \; n = 1, 2 \ldots N-1$$

where the $\bar{X}_g^{(n)}$ are mesh-interval-average values:

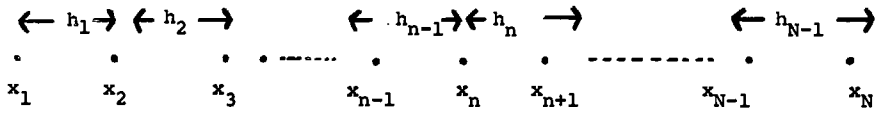

Fig. 3: Partition of the X-Dimension of a Reactor

$$\bar{X}_g^{(n)} \equiv \frac{1}{h_n} \int_{x_n}^{x_n + h_n} X_g(x) dx \qquad (1.36)$$

To express the derivatives at the end points of the intervals in terms of the $\bar{X}_g^{(n)}$ we account for the fact that, if $D_g^{(n-1)} \neq D_g^{(n)}$ these derivatives will be discontinuous at x_n. Accordingly, we use the two approximations

$$\frac{d}{dx} X_g(x) \Big|_{x_n^+} \simeq \frac{\bar{X}_g^{(n)} - X_g(x_n)}{(h_n/2)}$$

$$\frac{d}{dx} X_g(x) \Big|_{x_n^-} \simeq \frac{X_g(x_n) - \bar{X}_g^{(n-1)}}{(h_{n-1}/2)} \qquad (1.37)$$

Then since the normal current is continuous at x_n, we have

$$J_g(x_n) \simeq -D_g^{(n-1)} \frac{X_g(x_n) - \bar{X}_g^{(n-1)}}{(h_{n-1}/2)} = -D_g^{(n)} \frac{\bar{X}_g^{(n)} - X_g(x_n)}{(h_n/2)} \qquad (1.38)$$

Solving the last equation for $X_g(x_n)$ and substituting the result into either the left or the right hand side yields

$$J_g(x_n) = -D_g^n \frac{d}{dx} X_g(n) \Big|_{x_n^+} \simeq -\frac{2 D_g^{(n)} D_g^{(n-1)}}{D_g^{n-1} h_n + D_g^{(n)} h_{n-1}} (\bar{X}_g^{(n)} - \bar{X}_g^{(n-1)}) \qquad (1.39)$$

Substitution of this result into (1.35) then leads to the one-simensional, slab-geometry, mesh-centered finite difference equations:

$$\frac{2D_g^{(n)}D_g^{(n-1)}}{D_g^{(n-1)}h_n+D_g^{(n)}h_{n-1}}(\bar{X}_g^{(n)}-\bar{X}_g^{(n-1)}) - \frac{2D_g^{(n+1)}D_g^{(n)}}{D_g^{n}h_{n+1}+D_g^{(n+1)}h_n}(\bar{X}_g^{(n+1)}-\bar{X}_g^{(n)}) +$$

$$h_n(D_g^{(n)}B_{yz}^2+\Sigma_{tg}^{(n)})\bar{X}^{(n)} = \sum_{g'=1}^{G} h_n(\Sigma_{gg'}^{(n)}+\chi_g\nu\Sigma_{fg'}^{(n)})\bar{X}_{g'}^{(n)}$$

$$g = 1, 2, \ldots G;\ n = 1, 2, \ldots N-1 \qquad (1.40)$$

Boundary conditions at the outer surface of the reactor are easily accommodated. If, for example, $X_g(x_1) = 0$, we simply use the last term in (1.35) to approximate $J_g(x_1)$ in (1.35). Similarly, if $J_g(x_N) = 0$ we eliminate this term from (1.35) for $n = (N-1)$.

c) Solution of One-Dimensional Finite Difference Equations

Both sets of equations (1.34) and (1.40) are called "three point" difference equations, since at interior points the interface or average flux for each group ($X_g^{(n)}$ or $\bar{X}_g^{(n)}$) is connected only to its two nearest neighbors. For the first and last mesh point or interval only two neighboring fluxes appear.

From a mathematical point of view (1.34) and (1.40) represent sets of (respectively) G(N-2) and G(N-1) simultaneous, homogeneous, algebraic equations. If all terms are brought to the left hand side and the equations are written in matrix form the result can be expressed as

$$\underline{\underline{H}}\ \underline{X} = 0 \qquad (1.41)$$

where $\underline{X}$ is a G(N-2) or G(N-1) column vector of the unknown group fluxes and $\underline{\underline{H}}$ is a G(N-2) x G(N-2) or G(N-1) x G(N-1) matrix.

Equation (1.41) will have a non-trivial solution if and only if the determinant of $\underline{\underline{H}}$ vanishes. This mathematical condition is a reflection that the reactor will be critical only if the production rate of neutrons equals the destruction rate.

Rather than vary reactor loading, size or poison content to attain the critical condition it is much more satisfactory mathematically to attain criticality by dividing the fission production term by a positive real number λ (often called k_{eff}, "the effective multiplication constant" of the reactor). It is plausible and physical grounds that such a number λ can always be found, and it can be proved for finite difference approximations in one, two, and three dimensions and any number of energy groups that such is the case [1]. In face there are a number of values of λ (λ_0, λ_1, λ_2 ...) that can be found such that the determinant $|\underline{\underline{H}}| = 0$, and it can be proved that there is one real, positive, isolated λ-value (call it λ_0) such that $\lambda_0 > |\lambda_p|$; $p = 1, 2, \ldots$ Furthermore, the solution $\underline{X}_0$ associated with λ_0 is the only solution of (1.41) that has positive fluxes for all groups at all internal mesh points. Some of the elements $X_{gp}^{(n)}$ of the solution vectors $\underline{X}_p$ associated with λ_p's for $p \neq 0$ have signs differing from others; such $\underline{X}_p$'s do not correspond to physically acceptable solutions. It follows that, in attempting to solve (1.41) we shall be looking for λ_0 and $\underline{X}_0$.

The direct solution of (1.41) is not economical. Instead powerful iterative methods have been developed [1]. To illustrate we consider the mesh centered form (Eq. (1.40). With the definitions

$$\Sigma_g^{(n)} \equiv \Sigma_{tg}^{(n)} - \Sigma_{gg}^{(n)} \tag{1.42}$$

and the assumptions $\Sigma_{gg'}^{(n)} = 0$, $g' > g$, this equation may be written in the form

$$a_{n,n-1}\bar{X}_g^{(n-1)} + a_n\bar{X}_g^{(n)} + a_{n,n+1}\bar{X}_g^{(n+1)} = \sum_{g'<g} h_n\Sigma_{gg'}^{(n)}\bar{X}_{g'}^{(n)}$$

$$+ \sum_{g'=1}^{G} h_n\chi_g\nu\Sigma_{fg'}^{(n)}\bar{X}_{g'}^{(n)} \equiv S_g^{(n)} \tag{1.43}$$

where the $a_{n,n'}$ are defined by comparison with (1.40). (Note that $a_{10} = a_{N-1,N} = 0$ and all other $a_{nn'}$, $n \neq n'$ are negative.)

To solve (1.43) interatively we begin by guessing values for the $\bar{X}_{g'}^{(n)}$ which we shall label $\bar{X}_{g'}^{(n)}(0)$ and forming the fission source terms $\sum_{g'=1}^{G} h_n\chi_g\nu\Sigma_{fg'}^{(n)}\bar{X}_{g'}^{(n)}(0) \equiv S_{fg}^{(n)}(0)$ (normalized in some arbitrary fashion). Next, we solve (1.43 for the group-1 fluxes which we shall label $\bar{X}_1^{(n)}(1)$. (The scheme for doing this will be described below.) Then we compute the scattering-in terms $h_n\Sigma_{2'}^{(n)}\bar{X}_1^{(n)}(1)$ for group-2 and add them to the $S_{fg}^{(n)}(0)$. The $\bar{X}_2^{(n)}(1)$ can then be found, and the group-by-group solution continued down in energy until values for all the $\bar{X}_g^{(n)}(1)$ consistent with the initial fission source guess $S_{fg}^{(n)}(0)$ are found. This process is called an "outer iteration". We then find a first estimate of the eigenvalue $\lambda(1)(k_{eff})$ by forming the fission rate term $\sum_{g'=1}^{G} \nu\Sigma_{fg'}^{(n)}\bar{X}_{g'}^{(n)}(1)$ and then computing

$$\lambda(1) = \frac{\sum_{n,g'} \nu\Sigma_{fg'}^{(n)}\bar{X}_{g'}^{(n)}(1)}{\sum_{n,g'} \nu\Sigma_{fg'}^{(n)}\bar{X}_{g'}^{(n)}(0)} \tag{1.44}$$

An improved normalized fission source $S_{fg}^{(n)}(1)$ is then formed and the iteration process continues. When the fluxes and eigenvalues from two successive iterations differ by less than some prescribed amount the solution is said to be converged. It is possible to prove that this iteration process converges to the fundamental flux solution $\underline{X}_o$ and its corresponding eigenvalue $\lambda_o^{(1)}$.

The only part of the solution method that remains to be discussed concerns the solution of (1.43) for the $\bar{X}_g^{(n)}$'s. Written in matrix form this equation becomes

$$\underline{\underline{A}}\ \underline{\bar{X}}_g = \underline{S}_g \tag{1.45}$$

Where $\underline{\underline{A}}$ is an (N-1) x (N-1) "three stripe" matrix (see Eq. (1.46 below). To solve (1.45) we write $\underline{\underline{A}}$ as the product of two two-stripe matrices;

$$\underline{\underline{A}} = \begin{pmatrix} a_{11} & a_{12} & 0 & 0 \cdots \\ a_{21} & a_{22} & a_{23} & 0 \cdots \\ 0 & a_{32} & a_{33} & a_{34} \cdots \\ \vdots & \vdots & \vdots & \vdots \end{pmatrix} \equiv \begin{pmatrix} 1 & 0 & 0 & 0 \cdots \\ b_{21} & 1 & 0 & 0 \cdots \\ 0 & b_{32} & 1 & 0 \cdots \\ \vdots & \vdots & \vdots & \vdots \end{pmatrix} \begin{pmatrix} c_{11} & c_{12} & 0 & 0 \cdots \\ 0 & c_{22} & c_{23} & 0 \cdots \\ 0 & 0 & c_{33} & c_{34} \cdots \\ \vdots & \vdots & \vdots & \vdots \end{pmatrix} \tag{1.46}$$

Thus, multiplying the two component matrices, we obtain

$$\underline{\underline{A}} \equiv \underline{\underline{B}}\,\underline{\underline{C}} = \begin{pmatrix} c_{11} & c_{12} & 0 & 0 \cdots \\ b_{21}c_{11} & b_{21}c_{12}+c_{22} & c_{23} & 0 \cdots \\ 0 & b_{32}c_{22} & b_{32}c_{23}+c_{33} & c_{34} \cdots \\ \vdots & \vdots & \vdots & \vdots \end{pmatrix} \tag{1.47}$$

from which it follows that

$$c_{n,n+1} = a_{n,n+1}$$

$$c_{11} = a_{11}$$

$$b_{n,n-1} = \frac{a_{n,n-1}}{c_{n,n}} \; ; \; n > 1$$

$$c_{n,n} = a_{n,n} - b_{n,n-1}\, c_{n-1,n} \; ; \; n > 1 \tag{1.48}$$

Thus the elements of $\underline{\underline{B}}$ and $\underline{\underline{C}}$ can be found readily. Then to solve (1.45) we write

$$\underline{\underline{A}}\,\underline{\bar{X}}_g = \underline{\underline{B}}\,\underline{\underline{C}}\,\underline{\bar{X}}_g = \underline{S}_g \tag{1.49}$$

so that, defining $\underline{\bar{Y}}_g$ by

$$\underline{\bar{Y}}_g \equiv \underline{\underline{C}}\,\underline{\bar{X}}_g \tag{1.50}$$

we obtain

$$\underline{\underline{B}}\,\underline{\bar{Y}}_g = \underline{S}_g \tag{1.51}$$

This last equation can be solved easily. Multiplying out $\underline{\underline{B}}\,\underline{\bar{Y}}_g$ we find

$$\bar{Y}_g^{(1)} = S_g^{(1)}$$

$$\bar{Y}_g^{(n)} = S_g^{(n)} - b_{n,n-1}\, \bar{Y}_g^{(n-1)} \; ; \; n > 1 \tag{1.52}$$

Then, with the $\bar{Y}_g^{(n)}$ known, we obtain from (1.50)

$$\bar{X}_g^{(N-1)} = \frac{1}{C_{N-1,N-1}}\, \bar{Y}_g^{(N-1)}$$

$$X_g^n = \frac{\bar{Y}_g^n - c_{n,n-1}\, \bar{X}_g^{(n+1)}}{c_{n,n}} \tag{1.53}$$

Thus, we can determine all (N-1) of the $\bar{X}_g^{(n)}$'s by first sweeping down the mesh points (to find the $\bar{Y}_g^{(n)}$'s) and then sweeping back. This method for solving (1.45) is called "forward elimination, backward substitution".

d) Extension To More Dimensions

Extension of the finite difference method to more than one dimension is straight forward. We simply impose the approximate expressions (1.33) or (1.39) (relating net current across an interface to the fluxes on adjacent sides) to all faces of a mesh box. The result is a set of equations of the form (1.34) or (1.40) except that the flux in a given mesh box is now related (in two dimensions) to five nearest neighbors or (in three dimensions) to six nearest neighbors. The outer iteration scheme is the same as that described for the one-dimensional case. However, the matrix analogous to the 3-stripe matrix $\underline{\underline{A}}$ of Eq. (1.45) is now 5 or 7-stripe.

The solution $\underline{X}_g$ of (1.45) for $\underline{\underline{A}}$ a 5 or 7-stripe matrix cannot be found by the forward elimination, backward substitution method. Instead it is customary to use an iteration method. One such method that is used frequently is the "Gauss-Saidel" method [1]. The basic idea of this scheme is to split $\underline{\underline{A}}$ into a sum of a lower-triangular, a diagonal and an upper-triangular matrix:

$$\underline{\underline{A}} = \underline{\underline{L}} + \underline{\underline{D}} + \underline{\underline{U}} = \tag{1.54}$$

Then (1.45) is written

$$(\underline{\underline{L}} + \underline{\underline{D}})\ \bar{\underline{X}}_g = -\ \underline{\underline{U}}\ \bar{\underline{X}}_g + \underline{S}_g \tag{1.55}$$

With $\underline{S}_g$ known after a given outer iteration, we guess at $\bar{\underline{X}}_g$ on the right side (or use its most recently computed value) and solve for $\bar{\underline{X}}_g$ on the left hand side. This latter quantity can be found by a simple extension of the method employed to solve (2.1.51). Then the newer value of $\bar{\underline{X}}_g$ is multiplied by $\underline{\underline{U}}$, the result subtracted from $\underline{S}_g$, and the iteration process is continued to convergence. Such iterations are called "inner iterations". It can be proved that this iteration process will always converge for the finite difference form of the group diffusion equations [1].

The solution of the finite difference approximation to the group diffusion equations in two or three dimensions thus involves a double iteration. If several hundred thousand mesh points are involved the method can become quite expensive. Very sophisticated schemes have been devised to accelerate the convergence of both the outer and inner iteration procedures [1]. However, with upwards to a million unknown group-fluxes to be found, one does not ever expect the price of a calculation to become cheap.

1.3 Advanced Methods for Cores With Explicitly Represented Heterogeneities

If control rods or rod channels, burnable poison lumps, different zones of enrichment, structural materials between fuel assemblies, etc. are represented as explicit regions having individual group diffusion parameters, the finite difference solution of the group diffusion equations becomes extremely expensive. The reason is that the number of mesh points required to describe the geometry and provide a solution that approximates

accurately the analytical result can easily be several million.

We shall consider two classes of approximate methods for solving the group diffusion equations that retain the explicit geometrical detail but (at some cost in accuracy) reduce the computational cost. These schemes are the space-synthesis method and the response matrix method.

a) The Space Synthesis Method [2]

The space synthesis technique is based on the observation that reactors are generally fairly homogeneous in the axial direction. In fact about the only severe heterogeneities in the axial direction are due to partially inserted control rod banks and the boundaries of the core itself. Thus the 10 or 12 foot axial extension of a light water power reactor is generally composed of four or five regions which, although quite heterogeneous in the radial dimensions are (at any fixed radial point) homogeneous in the axial dimensions. Except at the axial interfaces of these regions it is plausible to assume that the group-g flux shape is approximately separable. Thus, within each axial zone we expect that

$$\phi_g(x,y,z) \approx \psi_k^g(x,y)\ T_k^g(z); \qquad (1.56)$$
$$z \text{ axial zone } k$$

where $\psi_k^g(x,y)$ is the two-dimensional group-g flux shape appropriate to the radial configuration of reactor materials in axial zone k.

Near the interface between zone (k) and (k + 1) we expect that $\phi_g(x,y,z)$ can be represented by some linear combination of $\psi_k^g(x,y)$ and $\psi_{k+1}^g(x,y)$. Thus throughout the entire reactor it is plausible to represent the group-g flux as

$$\phi_g(x,y,z) \approx \sum_{k=1}^{K} \psi_k^g(x,y)\ T_k^g(z)\ ; \qquad (1.57)$$
$$g = 1, 2, \ldots G \quad .$$

where the $T_k^g(z)$ are combining coefficients for the two dimensional flux shapes characteristic of various radial cuts through the reactor. If the axial level z is in the interior of, say, zone-p, we expect $T_p^g(z)$ will be much larger than all the other $T_k^g(z)$'s. Similarly, on the interface between zone-p and zone-(p+1) we expect that $T_p^g(z)$ and $T_{p+1}^g(z)$ will be about equal, both being larger than all the other $T_k^g(z)$'s.

If the approximation (1.57) is to be used, we must specify how to determine the expansion functions $\psi_k^g(x,y)$ and how to determine the combining coefficients $T_k^g(z)$.

We have already indicated how the $\psi_k^g(x,y)$ may be found. We merely solve the two dimensional version of (1.28) using group parameters (functions of x and y only) appropriate to the various axial zones and applying the finite difference method. It may be necessary to use in excess of 20,000 mesh points to provide the necessary geometrical detail over the radial planes.

However, the cost of running four or five - or even ten - such problems is far less than the cost of doing a single three dimensional problem involving, say, 20,000 x 100 = 2 x 10^6 mesh points.

Each of the computations run to find the $\psi_k^g(x,y)$ in the core region are eigenvalue problems and lead to values of k_{eff} necessary to make the various radial slices critical in the absence of the axial leakage of neutrons. For the axial reflector zones this technique for finding the expansion functions is not possible since the $\nu\Sigma_{fg}$ vanish in the reflector zones. Instead we find the $\psi_k^g(x,y)$ for the reflectors by solving a fixed source problem, the source being the fission source of the adjacent core region. Thus, if $\psi_o^g(x,y)$ is the desired expansion function typical of the reflector zone and $\psi_1^g(x,y)$ is the (previously found) corresponding expansion function for the adjacent core region, we solve the following reduced version of (1.28)

$$-\nabla\cdot D_o^g(x,y)\nabla\psi_o^g(x,y) + \Sigma_o^g(x,y)\psi_o^g(x,y) - \sum_{g'<g} \Sigma_o^{gg'}(x,y)\psi_o^{g'}(x,y)$$

$$= \sum_{g'=1}^{G} \chi_g \nu\Sigma_f^{g'} \psi_1^{g'}(x,y) \qquad (1.58)$$

where subscripts o or 1 on the group parameters indicate the region to which they belong. (Also note that the definition (1.42) has been applied.) Since the right hand side of (1.58) is known, only one outer iteration is required to determine the $\psi_o^g(x,y)$.

To find the one-dimensional "mixing functions" $T_k^g(z)$ we shall use the weighted residual method. The basic idea of this procedure is to recognize that the approximation 1.57) for $\phi_g(\underline{r})$ cannot in general be a valid solution of the group diffusion equation (1.28) for all points $\underline{r}$. However, we can force it to be a solution in a weighted integral sense. Thus, to determine the $T_k^g(z)$ we substitute (1.57) into (1.28), multiply by K different G-group weight functions $W_p^g(x,y)$; p = 1, ... K; g = 1, 2 or G, and integrate over the XY plane. The result will be KG coupled, one-dimensional equations in the KG mixing functions $T_k^g(z)$.

To show the algebraic details of this procedure it will be convenient to represent the group equations in matrix form. Accordingly we define the following GxG matrices by indicating their gg' elements in brackets { } :

$$\underline{\underline{D}}(\underline{r}) \equiv \text{Diag} \quad \{ D_g(\underline{r}) \}$$

$$\underline{\underline{A}}(\underline{r}) \equiv \{ \Sigma_{tg}(\underline{r})\delta_{gg'} - \Sigma_{gg'}(\underline{r}) \} \qquad (1.59)$$

$$\underline{\underline{M}}(\underline{r}) \equiv \{ \chi_g \nu\Sigma_{fg'}(\underline{r}) \}$$

Then, if the G-element column vector $\underline{\phi}(\underline{r})$ is defined by

$$\underline{\phi}(\underline{r}) \equiv \text{Col} \quad \{ \phi_g(\underline{r}) \} \qquad (1.60)$$

Equation (1.28) may be written

$$-\nabla\cdot\underline{\underline{D}}(\underline{r})\nabla\underline{\phi}(\underline{r}) + \underline{\underline{A}}(\underline{r})\underline{\phi}(\underline{r}) = \frac{1}{\lambda}\,\underline{\underline{M}}(\underline{r})\underline{\phi}(\underline{r}) \qquad (1.61)$$

where we have introduced the eigenvalue λ explicitly.

If, finally, we define diagonal GxG matrices of expansion and weight functions and a column vector of mixing coefficients by

$$\begin{aligned}
\underline{\underline{\psi}}_k(x,y) &\equiv \text{Diag}\ \{\psi_k^g(x,y)\}\\
\underline{\underline{W}}_k(x,y) &\equiv \text{Diag}\ \{W_k^g(x,y)\}\\
\underline{T}_k(z) &\equiv \text{Col}\ \{T_k^g(z)\}
\end{aligned} \qquad (1.62)$$

$$k = 1, 2, \ldots K$$

Equation (1.57) becomes

$$\underline{\phi}(x,y,z) \simeq \sum_{k=1}^{K} \underline{\underline{\psi}}_k(x,y)\,\underline{T}_k(z) \qquad (1.63)$$

The weighted residual procedure then consists of substituting (1.63) into (1.61), multiplying by the K weight matrices $\underline{\underline{W}}_k(x,y)$ and integrating over the XY domain of the reactor. The result is

$$-\sum_{k=1}^{K}\frac{\partial}{\partial z}\left[\int_{XY}\underline{\underline{W}}_p(x,y)\,\underline{\underline{D}}(\underline{r})\,\underline{\underline{\psi}}_k(x,y)\right]\frac{\partial}{\partial z}\underline{T}_k(z)$$

$$+\sum_{k=1}^{K}\left[\int_{XY}\underline{\underline{W}}_p(x,y)\ \left\{-\frac{\partial}{\partial x}\underline{\underline{D}}(\underline{r})\,\frac{\partial}{\partial x}\,\underline{\underline{\psi}}_k(x,y)\right.\right.$$

$$\left.\left.-\frac{\partial}{\partial y}\underline{\underline{D}}(\underline{r})\,\frac{\partial}{\partial y}\,\underline{\underline{\psi}}_k(x,y)+\underline{\underline{A}}(\underline{r})\,\underline{\underline{\psi}}_k(x,y)\right\}\right]\underline{T}_k(z) \;=$$

$$=\frac{1}{\lambda}\sum_{k=1}^{K}\left[\int_{XY}\underline{\underline{W}}_p(x,y)\,\underline{\underline{M}}(\underline{r})\,\underline{\underline{\psi}}_k(x,y)\right]\underline{T}_k(z)\ ;$$

$$p = 1, 2, \ldots K \qquad (1.64)$$

This equation may be rewritten in simpler notation as

$$-\sum_{k=1}^{K}\frac{\partial}{\partial y}\,\underline{\underline{D}}_{pk}(z)\,\frac{\partial}{\partial z}\,\underline{T}_k(z)+\sum_{k=1}^{K}\underline{\underline{A}}_{pk}(z)\,\underline{T}_k(z) =$$

$$=\frac{1}{\lambda}\sum_{k=1}^{K}\underline{\underline{M}}_{pk}(z)\,T_k(z)\ ;$$

$$p = 1, 2, \ldots K \qquad (1.65)$$

where the GxG matrices $\underline{\underline{D}}_{pk}$, $\underline{\underline{A}}_{pk}$ and $\underline{\underline{M}}_{pk}$ are defined by comparisor with (1.64).

Finally, (1.65) may be written in the "supermatrix" form

$$-\frac{\partial}{\partial z}\,\underline{\underline{D}}(z)\,\frac{\partial}{\partial z}\,\underline{T}(z)+\underline{\underline{A}}(z)\,\underline{T}(z)=\frac{1}{\lambda}\,\underline{\underline{M}}(z)\,\underline{T}(z); \qquad (1.66)$$

where $\underline{\underline{D}}(z)$ is a KxK supermatrix having the GxG matrix $\underline{\underline{D}}_{pk}(z)$ as its $(pk)^{th}$ element (similarly for $\underline{\underline{A}}$ and $\underline{\underline{M}}$) and $\underline{T}(z)$ is a K-element column vector having as its k^{th} element the G-element

vector $\underline{T}_k(z)$. In this supermatrix form the equation for the mixing coefficient vector $\underline{T}(z)$ can be seen to be a matrix generalization of the one-group diffusion equations 1.30 for G = 1), and, in fact, a matrix generalization of the forward elimination backward substitution technique can be used to solve (1.66).

We have not yet considered the problem of selecting the GxG weight function matrices $\underline{W}_p$; p = 1, 2, ... K. A derivation of (1.66) based on a variational principle suggests that the adjoint functions (see Section 2 of these notes) corresponding to the $\underline{\psi}_k$ are the favored choice [3]. However it has been found that the spatial shapes of the regular and adjoint fluxes for a given group do not differ significantly, and using the $\underline{\psi}_k$ themselves for the $\underline{W}_p$ usually produces just as accurate results. Moreover, with the $\underline{\psi}_k$ used for the $\underline{W}_k$ the cost of solving an extra set of two dimensional difference equations is avoided. This procedure is called "Galerkin weighting".

Many variants of the continuous space synthesis approximation have been investigated (see Ref. 3, Chapter 11, and Ref. 4). For example, in the "collapsed group approximation" the group-to-group ratios of the expansion and weighting matrices are assumed to be fixed ($T_k^g(z)/(T_k^{G+1}(z)$ = constant). Thus, (1.63) becomes

$$\underline{\phi}(x,y,x) = \sum_{k=1}^{K} \underline{\psi}_k(x,y)\ T_k(z) \qquad (1.67)$$

where $\underline{\psi}_k(x,y)$ is a G-element column vector and $T_k(z)$ is a scalar. The weight function matrices $\underline{W}_k$ (1.62) become row vectors (the transposes of column vectors $\underline{W}_k$), and the size of the matrices in (1.66) is reduced from (GK)x(GK) to KxK. If the collapsed group approximation is made, it is important that the group-to-group ratios of the $\underline{W}_k$ approximate those of the fluxes adjoint to the $\underline{\psi}_k$. This is because, although adjoint and regular flux shapes for a given group are similar, the group-to-group ratios are usually very different.

Another variant of the space-synthesis approach is known as "multichannel synthesis"[5]. In this approximation the $\underline{\psi}_k(x,y)$ are partitioned into several segments over the XY plane and the individual segments are treated as independent expansion functions. For example, the portions of the $\underline{\psi}_k(x,y)$ belonging to the four quadrants of the XY plane may be allowed to vary independently. The effects of flux tilting can then be accommodated without introducing special, tilted functions. The discontinuities in radial flux shapes that result from the approximation can be avoided by defining expansion functions as $f_n(x,y)\underline{\psi}_k(x,y)$; n = 1, 2, ... N; where the $f_n(x,y)$ are scalar functions equal to unity over most of the region where we wish $\underline{\psi}_k$ to be non-zero but then drop in a continuous fashion to zero throughout the rest of the core [6]. Figure 4 shows a sketch of two such functions for a one-dimensional slab of thickness L.

One final variant of the space synthesis scheme is called "discontinuous space synthesis"[7]. The basic idea of this method is to discard expansion functions in regions where they are not needed. For example, if ten radial $\underline{\psi}_k(x,y)$'s are

needed to account for all the different radial conditions in the core, we use perhaps only three of them at a given axial location.

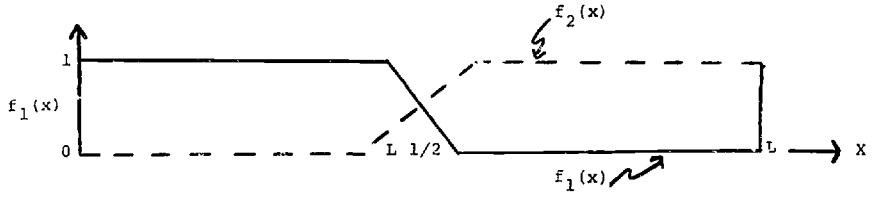

Fig. 4: Modulating Functions for a One Dimensional Situation

Thus, for z in the axial range where $\underline{\psi}_n$ is expected to dominate we use only $\underline{\psi}_{n-1}$, $\underline{\psi}_n$ and $\underline{\psi}_{n+1}$, in (1.62). Then when z moves to zone n+1 we discard $\underline{\psi}_{n-1}$ and add $\underline{\psi}_{n+2}$ in its place. Thus, although a total of ten expansion functional are used for the overall calculation, only three are used at any given Z-location. As a result in (1.62) K = 3 rather than 10, and (1.66) is simplified accordingly.

Flux synthesis methods have been found to be accurate and relatively inexpensive. However, they have several drawbacks. First of all, implementation by a computer program is very complicated. Secondly, there is no automatic way to select expansion functions that are guaranteed to be optimal. Physical insight and experience must be used, and if some physical behavior such as a flux tilt is not anticipated so that tilted expansion functions are not supplied, results can be seriously in error. Finally, there is no way to establish error bounds. Adding more mesh points in the case of finite difference approximation can be proved to improve accuracy; for synthesis methods increasing the number of expansion functions may actually reduce accuracy. These difficulties suggest that space synthesis procedures are best applied to problems for which the qualitative behavior of flux shapes is well understood. For such cases the method provides reliable and very detailed information about criticality and flux distribution throughout a geometrically complicated reactor.

b) Response Matrix Techniques

In the response matrix technique the reactor is partitioned into a number of fairly large subregions called nodes, and the "partial neutron currents" crossing the faces of these nodes from inside to outside and from outside to inside are treated as unknowns. Preliminary calculations are performed for each different node to determine "response matrix elements" specifying the neutron currents emerging from a given face of the node due to unit currents entering each of the nodal faces. The physical fact that currents emerging from one face of a node must equal those entering the adjacent face of the neighboring node is then applied to derive a set of equations connecting all the partial currents.

To describe the method in more quantitative detail we first define a "partial current density" mathematically and show its relationship to the scalar flux density and the net current density. Thus we define $J_z^+(r,E)\,dE$ as the number of neutrons

per second with energies in dE crossing a unit surface perpendicular to the Z-axis and containing point $\underline{r}$ from the negative side (z less than the Z-componet of $\underline{r}$) to the positive side (z greater than the Z-component of $\underline{r}$). The partial current $J_z^-(\underline{r},E)dE$ is defined similarly except that it refers to neutrons crossing from the positive to the negative side of the unit surface. Analogous partial currents $J_x^{\pm}$ and $J_y^{\pm}$ are defined for unit surfaces perpendicular to the X and Y axis. It follows that the net current in the three coordinate directions are

$$J_u(\underline{r},E) = J_u^+(\underline{r},E) - J_u^-(\underline{r},E);\ u = X,Y,Z$$

$$= \int_{\Omega} \Omega_u v(E)N(r,\underline{r},E)d\Omega$$

the latter expression coming from Eq. (1.14).

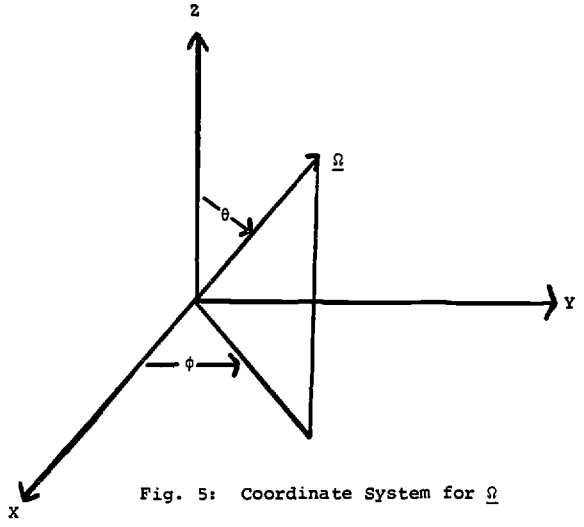

Fig. 5: Coordinate System for $\underline{\Omega}$

It also follows from the definitions of the $J_u^{\pm}$ that we find these quantities by integrating $\Omega_u v(E)N(r,\underline{r},E)$ over a hemisphere rather than over the entire sphere. Thus, for $\underline{\Omega}$ expressed in spherical coordinates (Fig. 5) we have

$$J_z^+(\underline{r},E) = \frac{1}{4\pi}\int_o^{2\pi}d\phi \int_o^{\frac{\pi}{2}} \sin\theta d\theta\ \Omega_z v(E)N(\underline{r},\underline{\Omega},E) \qquad (1.69a)$$

If we then approximate vN by the P-1 expression (1.15) J_z^+ becomes

$$J_z^+(\underline{r},E) = \frac{1}{4\pi}\int_o^{2\pi}d\phi \int_o^{\frac{\pi}{2}}d\theta\ \sin\theta\ \cos\theta \Big[\phi(\underline{r},E) +$$

$$3(\sin\theta\cos\phi\ J_x(\underline{r},E) + \sin\theta\sin\phi\ J_y(\underline{r},E)$$

$$+ \cos\theta\ J_z(\underline{r},E)\Big] \quad = \frac{1}{4}\phi(\underline{r},E) + \frac{1}{2}J_z(\underline{r},E) \qquad (1.69b)$$

Similar calculations show that, in general, for the P-1 approximation, partial currents are related to net currents by

$$J_u^{\pm}(\underline{r},E) = \frac{1}{4}\phi(\underline{r},E) \pm \frac{1}{2}J_u(\underline{r},E);\quad u = x,y,z \qquad (1.70)$$

By adding and subtracting J_u^+ and J_u^- we find the inverse relationships

$$\phi(\underline{r},E) = 2\left[J_u^+(\underline{r},E) + J_u^-(\underline{r},E)\right]$$

$$J_u(r,E) = J_u^+(\underline{r},E) - J_u^-(\underline{r},E) \qquad (1.71)$$

These relationships can lead to mathematical problems at points where the material properties of the medium are discontinuous. Since we shall avoid these difficulties, they will not be discussed explicitly.

The next step in the response matrix procedure is to define response matrix elements. Roughly these are the partial currents of group-g neutrons emerging from face-n of the node due to a partial current of group-g' neutrons entering across face-n', where face-n' can be face-n itself or any other face of the node. We shall designate this matrix element as $R_{nn'}^{gg'}$. To be precise we must specify the spatial and angular shapes of the entering and emerging current distributions. For the moment, however, let us make the simplest approximation, namely, that the spatial distribution of entering currents is flat along the respective faces of the node and that the angular distribution is isotropic over the entering hemispheres. Note that, even if the entering current distributions are spatially flat and isotropic in angle, the corresponding exiting quantities will not be. For the moment we shall nevertheless assume they are.

With these approximations we can relate $J_n^g(\text{out})$ the average partial current of group-g neutrons emerging from face-n due to group-g' currents entering faces-n' ($J_{n'}^{g'}(\text{in})$) by

$$J_n^g(\text{out}) = \sum_{n'g'} R_{nn'}^{gg'} J_{n'}^{g'}(\text{in}); \qquad n = 1, 2, \ldots N;\ g = 1, 2, \ldots G \tag{1.72}$$

If all the $J_n^g(\text{out})$'s and $J_n^g(\text{in})$'s are assembled into column vectors, $\underline{J}(\text{out})$ and $\underline{J}(\text{in})$, Eq. (1.72) can be written as a single matrix equation

$$\underline{J}(\text{out}) = \underline{\underline{R}}\ \underline{J}(\text{in}) \tag{1.73}$$

Moreover, since the $J_n^g(\text{out})$ of one node equal the $J_{n'}^g(\text{in})$ of adjacent nodes, the vector $\underline{J}(\text{in})$ is simply a rearrangement of the vector $\underline{J}(\text{out})$,

$$\underline{J}(\text{in}) = \underline{\underline{A}}\ \underline{J}(\text{out}) \tag{1.74}$$

where $\underline{\underline{A}}$ is a permutation matrix.

Thus the $\underline{J}(\text{out})$'s are solutions of the eigenvalue problem

$$\gamma\ \underline{J}(\text{out}) = \underline{\underline{R}}\ \underline{\underline{A}}\ \underline{J}(\text{out}) \tag{1.75}$$

where γ is an eigenvalue introduced to insure a non-trivial solution (analogous to the λ of Eq. (1.61). The matrix $\underline{\underline{R}}\ \underline{\underline{A}}$ is non-negative and irreducible. Under those conditions it is possible to prove [2] that there exists a simple eigenvalue γ equal to the spectral radius of $\underline{\underline{R}}\ \underline{\underline{A}}$ and that the corresponding eigenvalue is unique and has all positive entries. This is the solution we seek. For $\gamma = 1$, the reactor is exactly critical; for $\gamma > 1$ it is supercritical and for $\gamma < 1$ it is subcritical. If one wishes to find the more familiar eigenvalue λ (k_{eff}) by the response matrix procedure it is necessary to divide the

values of $\nu\Sigma_f$ used to determine $\underline{R}$ (see below) by a succession of numbers, λ, until that λ is found for which $\gamma = 1$. This search procedure is time consuming, and it is difficult to see what is gained by it.

To determine the $R_{nn'}^{gg'}$, auxiliary computations must be carried out for each different node making up the reactor. The node is isolated in a vacuum; a source of group-g' neutrons is allowed to impinge on face-n', and the group-g neutron currents emerging from all faces are computed. By definition these are the $R_{nn'}^{gg'}$ for inlet and outlet neutron beams assumed spatially flat and isotropic over the inward or outward directed hemispheres. It should be noted that any augmentation of the neutron population due to fission is accounted for by this way of finding the $R_{nn'}^{gg'}$. Also, most important, there is no need that the nodes be homogeneous nor that the nodal calculation be carried out in the diffusion theory approximation. Sophisticated transport theory methods can be used to compute response matrices [8]. Since these methods need be applied to only a few different kinds of nodes rather than over the whole reactor, the computing cost of finding the $R_{nn'}^{gg'}$ is not prohibitive. Also, since the nodes are large in size, there may be only several thousand of them. Thus, the solution of (1.75) is manageable.

The major drawback to the response matrix technique involves the assumptions about the spatial and angular distributions of the neutrons making up the incoming and outgoing partial currents. We have so far assumed flat shapes and isotropic angular distributions over the entering and exiting hemispheres. But this restriction is not necessary in principle. Entering and exiting currents can be decomposed into any number of fixed spatial and angular shapes [9] and response matrix elements $R_{nn';ss'}^{gg';aa'}$ computed specifying the number of group-g neutrons emerging from face-n having angular distribution-a and spatial shape-s due to a unit incoming current of group-g' neutrons entering face-n' with angular distribution-a' and spatial shape-s'. The trouble with this generalization is that the magnitude of the calculations quickly gets out of hand. Use of only two angular and two spatial distributions on each face of a node increases the number of unknowns in $\underline{J}$(in) and $\underline{J}$(out) by a factor of 4 and the number of matrix elements by a factor of 16. Thus the practical utility of the response matrix method depends on how well the spatial and angular shapes of the neutrons entering and leaving the faces of the nodes can be represented by a single function or by a combination of a very few functions. If this number can be kept small the method can account for both geometrical complexity and transport theory phenomena within the nodes.

1.4 Methods for Cores Represented by Large Homogenized Nodes

The finite difference, synthesis and response matrix procedures are all directly applicable to the analysis of reactors composed of heterogeneous assemblies such as the one shown in Figure (2). Except with the response matrix technique it is necessary to have group-diffusion parameters for each explicit region when these methods are applied. Methods for determining these group-diffusion theory parameters have been discussed in the first week of this course. We shall call these methods the

"first stage" of homogenization. Homogenized group-diffusion parameters representing fuel rod cells (composed of a fuel rod, its cladding and associated moderator), control rod material, structural zones (possibly mixtures of coolant and metal), and lumps of burnable poison (and associated structural material) result from this first stage of homogenization. A group-diffusion theory model in which a very large number of different material regions are represented explicitly results, and a very large number of mesh points must be used just to describe the geometry of the reactor.

In order to reduce the number and - more important - in order to permit the application of more efficient computational methods a second stage of homogenization is often carried out. This second stage of homogenization is usually accomplished by a simple flux weighting procedure, although recently more sophisticated methods have been suggested [10,11]. In the flux weighting homogenization scheme a detailed flux computation is performed for a large heterogeneous node (such as a 20 cm axial section of a fuel assembly) with zero current boundary conditions applied over the surface of the node. The resultant flux shapes $\phi_g(\underline{r})$ for the various groups are used to find average group parameters $\bar{\Sigma}_{\alpha g}$ (α standing for fission, absorption or scattering) according to the formula

$$\bar{\Sigma}_{\alpha g} = \frac{\int_V \Sigma_{\alpha g}(\underline{r})\ \phi_g(\underline{r})\ dV}{\int_V \phi_g(\underline{r})\ dV} \qquad (1.76)$$

where the volume integral is over the heterogeneous node. The diffusion coefficients $\bar{D}_g$ are usually found in the same manner.

If homogenized group-diffusion parameters for the reactor nodes are found by the two stage homogenization procedures, the final mathematical model of the reactor is one composed of large homogeneous zones. If finite difference solutions are carried out, the number of mesh regions required is now determined by the accuracy of the finite difference approximation (Eq. 1.33) and (1.39) rather than by the geometry. For light water reactors the nodes will be of size ~ 20 cm by 20 cm in the radial plane. But accuracy may require use of mesh spacings of less than a centimeter near the core-reflector interface and of no more than 3 or 4 cm in the interior. The situation suggests that approximation methods be used that require a fewer number of unknowns for a given accuracy than the number needed for the finite difference approximation. We shall outline two classes of such methods: finite element techniques and nodal methods.

a) Finite Element Techniques

With the group diffusion theory parameters constant throughout each node it is expected that flux shapes within the nodes will be fairly smooth. This fact in turn suggests that the flux shapes within the nodes could be approximated well by polynomials. The finite element method is a systematic way of making such an expansion. Its chief distinguishing feature is that the polynomial have "local support"; that is, they are zero over all but small regions of the reactor (usually a node and its nearest neighbors). Thus the group-g flux is expressed

as

$$\phi_g(x,y,z) \approx \sum_{k=1}^{K} P_g^{(k)}(x,y,z) \equiv \phi_g^{(a)}(\underline{r}) \tag{1.77}$$

where the P_k are continuous functions composed of polynomials of a certain value in x,y,and z. Each $P_g^{(k)}$ is now zero over only a small portion of the reactor (although regions where the polynomials are non-zero may overlap).

The unknowns of the problem are the coefficients of the $P_g^{(k)}$. These may be found by a weighted residual method. Thus we substitute the approximation $\phi_g^{(a)}(\underline{r})$ into (1.28), weight by a sequence of weight functions $W_g^{(n)}(\underline{r})$ (equal in number to the number of unknowns in $\phi_g^{(a)}$) and require the result to be true when integrated over the reactor:

$$\int W_g^{(n)}(\underline{r}) \{ -\nabla \cdot D_g(\underline{r}) \nabla \phi_g^{(a)}(\underline{r}) + \Sigma_{tg}(\underline{r}) \phi_g^{(a)}(\underline{r}) - \sum_{g'=1}^{G} \left[\Sigma_{gg'}(\underline{r}) + \chi_g \nu \Sigma_{tg'}(\underline{r}) \right] \phi_{g'}^{(a)}(\underline{r}) \} \, dV = 0 \; ; \quad g = 1, 2, \ldots, G \tag{1.78}$$

We shall restrict our solution of trial and weight functions so that $\phi_g^{(a)}(\underline{r})$ and the $W_g^{(n)}(\underline{r})$ are continuous and vanish on the outer surface of the reactor, and, for the moment, we shall also assume that the normal component of the $D_g(\underline{r}) \nabla \phi_g^{(a)}(\underline{r})$ are also continuous across internal interfaces between nodes. Then, since

$$\nabla \cdot \left[W_g^{(n)}(r) D_g(\underline{r}) \nabla \phi_g^{(a)}(\underline{r}) \right] = W_g^{(n)}(\underline{r}) \nabla \cdot \left[D_g(\underline{r}) \nabla \phi_g^{(a)}(\underline{r}) \right] + \left[\nabla W_g^{(n)}(\underline{r}) \right] \cdot \left[D_g(\underline{r}) \nabla \phi_g^{(a)}(\underline{r}) \right] \tag{1.79}$$

and (since $W_g^{(n)}(\underline{r}) = 0$ on the outer surface S_o).

$$\int_V \nabla \cdot \left[W_g^{(n)} D_g \nabla \phi_g^{(a)} \right] = \int_{S_o} \left[W_g^{(n)} D_g \nabla \phi_g^{(a)} \right] \cdot n dS_o = 0 \tag{1.80}$$

and the volume integrals of the two terms on the right hand side of (1.79) are equal and opposite in sign. Thus (1.78) becomes

$$\int \{ \nabla W_g^{(n)} \cdot D_g \nabla \phi_g^{(a)} + W_g^{(n)} \Sigma_{tg} \phi_g^{(a)} - W_g^{(n)} \sum_{g'=1}^{G} \left[\Sigma_{gg'} + \chi_g \nu \Sigma_{fg'} \right] \phi_g^{(a)} \} \, dV = 0 \tag{1.81}$$

We have derived the result under the assumption that the normal components of $D_g \nabla \phi_g^{(a)}$ are continuous across internal interfaces. Actually the limitation is not necessary. The expression can be derived under the weaker assumption only that

$\phi_g^{(a)}(\underline{r})$ and the $W_g^{(n)}(\underline{r})$ are continuous and vanish on S_o (see Ref. 3, p. 500). For that space of functions (1.81) is known as the "weak form" of the group diffusion equations.

To illustrate the finite element method we shall consider the very simple example of an expansion in linear functions for one-dimensional slab geometry. For this case we take

$$p_g^k(x) = \begin{cases} \dfrac{x_{k+1} - x}{h_k}\ \phi_g^{(k)} & \text{for } x_k \le x \le x_{k+1} \\ \dfrac{x - x_k}{h_{k-1}}\ \phi_g^{(k)} & \text{for } x_{k-1} \le x \le x_k \\ 0 \text{ for all other } x \end{cases} \qquad (1.82)$$

where the mesh layout is as shown in Fig. 3, all interfaces across which material properties change being one of the x_k's and material properties being constant within each mesh interval h_k. Two expansion functions $p_g^k(x)$ and $p_g^{(k+1)}(x)$ and a segment of the overall flux shape $\phi_g^{(a)}$ formed from them according to (1.77) is shown in Fig. 6. The composite function $\phi_g^{(a)}(x)$ in the range $x_a \le x \le x_{k+1}$ is formed by the sum of the two overlapping "tent functions" shown in the top of the figure, all other expansion functions $P_g^n(x)$; $n \neq k$, k+1 being zero in that range.

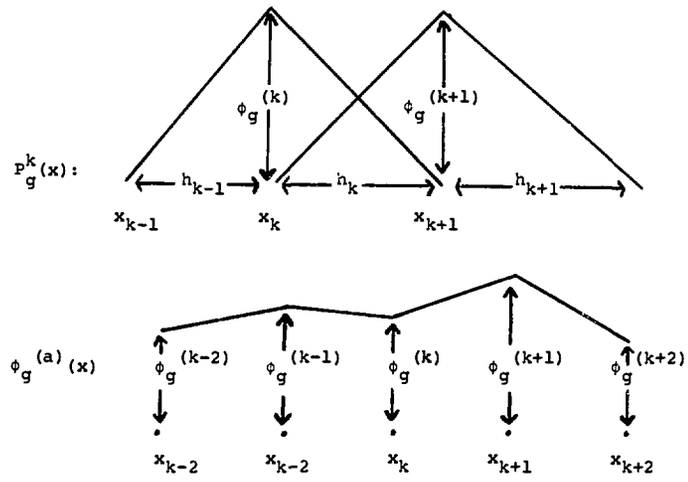

Fig. 6: Expansion Function $p_g^k(x)$ and Segment of $\phi_g^{(a)}(x)$

To determine the $\phi_g^{(k)}$ we approximate as in (1.77)

$$\phi_g^{(a)}(x) \approx \sum_{k=1}^{N-1} P_g^{(k)}(x) \qquad (1.83)$$

and, substitute this result into (1.81) using (1.82) to represent the $P_g^R(x)$. If we use normalized tent functions $\dfrac{P_g^n(x)}{\phi_g^n}$; n = 1, 2 ... N-1 as weight functions $W_g^{(n)}(x)$,

Eq. (1.81) will yield exactly G(N-1) equations for the G(N-1) unknown $\phi_g^{(n)}$'s. Note that for a fixed $W_g^{(n)}(x)$ only three $P_g^{(k)}(x)$ in the sum 1.83) survive. The result of performing the differentiation and integration indicated for (1.81) is

$$\frac{1}{h_{k-1}} D_g^{(k-1)} (\phi_g^{(k)} - \phi_g^{(k-1)}) - \frac{1}{h_k} D_g^{(k)} (\phi_{g+1}^{(k)} - \phi_g^{(k)}) +$$

$$+ h_{k-1} \left[\Sigma_{tg}^{(h-1)} (\tfrac{1}{3}\phi_g^{(k)} + \tfrac{1}{6}\phi_g^{(k-1)}) - \right.$$

(Eq. continued)

$$\left. - \sum_{g'=1}^{G} (\Sigma_{gg'}^{(k-1)} + \chi_g \nu\Sigma_{fg'}^{(k-1)}) (\tfrac{1}{3}\phi_{g'}^{(k)} + \tfrac{1}{6}\phi_{g'}^{(k-1)}) \right]$$

$$+ h_k \left[\Sigma_{tg}^{k} (\tfrac{1}{3}\phi_g^{k} + \tfrac{1}{6}\phi_g^{k+1} - \sum_{g'=1}^{G} (\Sigma_{gg'}^{k} + \chi_g \nu\Sigma_{fg'}^{k}) (\tfrac{1}{3}\phi_{g'}^{(k)} + \tfrac{1}{6}\phi_{g'}^{(k+1)}) \right]$$

$$= 0; \quad k = 1, 2, \ldots N-1 \qquad (1.84)$$

Note the similarity of this equation to the finite difference result (1.34). Both theoretically and empirically the finite element result can be shown to be more accurate. Thus, for a given degree of accuracy, larger values of h_k (and hence fewer mesh points) can be used with the finite element equations.

Still greater accuracy can be achieved by using higher order polynomials. For example, a set of three cubic polynomials $P_g^{(k)o}(x)$, $P_g^{(k)+}(x)$, $P_g^{(k)-}(x)$ can be associated with mesh point k, where $P_g^{(k)(0)}(x)$ vanishes for $x \leq x_{k-1}$; $x \geq x_{k+1}$, has the value $\phi_g^{(k)}$ at $x = x_k$ and has zero derivative at x_{k-1}, x_k and x_{k+1}; $P_g^{(k)+}(x)$ vanishes for $x \leq x_k$; $x \geq x_{k+1}$ has a derivative $\frac{d\phi_g}{dx}\Big|_{x_k+}$ for x on the (+) side of x_k and a zero derivative at x_{k+1}, and $P_g^{(k)-}(x)$ vanishes for $x_{k-1} \leq x \leq x_k$, has a derivation $\frac{d\phi}{dx}\Big|_{x_k-}$ for x on the (-) side of x_k and a zero derivative at x_{k-1}. (These functions are called cubic Hermite polynomials.) There are then 3G unknown coefficients at each mesh point, and the finite element equations analogous to (1.85) are more complicated. On the other hand, the equations are more accurate so that fewer mesh points are required.

In two and three dimensions products of the one-dimensional polynomials may be used. Coupling becomes more extensive than for the finite difference case. For example, the extension to three dimensions using expansion functions that are products of the functions (1.82), one for each dimension, yields difference equations for which one mesh point is connected to 26 neighbors rather than to 8. For this linear case, however, the total number of unknowns is the same - namely, the $\phi_g(x_k\ y_k\ z_k)$, and in general it is found that far fewer unknowns are required for a finite element representation of the flux than for a finite difference representation of equal accuracy.

The question of whether there is a net savings realized by use of the finite element method (which involves fewer unknowns but a much greater degree of coupling) seems to be unsettled at the moment. Different groups have come to different conclusions [12, 13]. Thus, it is not clear at this time whether the finite element scheme actually can realize the great reduction in computing costs that would be expected from the reduction in the number of unknowns. Two other points, however, are not in dispute. The method does provide continuous values of the group fluxes throughout the reactor (not just at the mesh points) and decreasing mesh spacing improves the accuracy of the answer.

b) Nodal Methods

In nodal methods the primary unknowns are taken to be the average fluxes in the various nodes. The basic equation for such methods is then obtained by integrating (1.24) over the volume V_n of the n^{th} node (n = 1, 2, ... N). If we assume that the group parameters are constant throughout each node and designate them as $\Sigma_{tg}^{(n)}$, $\Sigma_{gg'}^{(n)}$ etc., we obtain

$$\frac{1}{V_n}\int_{S_n}\underline{J}_g\cdot\underline{n}\,dS + \Sigma_{tg}^{(n)}\,\bar{\phi}_g^{(n)} = \sum_{g'=1}^{G}\left[\Sigma_{gg'}^{(n)} + \chi_g\nu\Sigma_{fg'}^{(n)}\right]\bar{\phi}_{g'}^{(n)} \qquad (1.85)$$

where the average nodal flux for group-g is defined as

$$\bar{\phi}_g^{(n)} = \frac{1}{V_n}\int_{V_n}\phi_g(\underline{r})\,dV \qquad (1.86)$$

The various nodal schemes differ from each other through the ways that currents across surfaces between nodes are related to the average fluxes in those nodes. The older nodal schemes [14, 15] establish this relationship by using escape probability arguments. More recently, for Cartesian geometries, a new class of nodal schemes have been developed [16, 17, 18]. These methods are based on relating the $\underline{J}_g\cdot n$'s across a given nodal face to the adjacent $\bar{\phi}_g^{(n)}$'s through the solution of average one-dimensional equations. To indicate how this is done we shall examine the two dimensional case.

Thus we consider a rectangular node of size $h_i^{(x)} \times h_j^{(y)}$ ($h_i^x \equiv (x_{i+1} - x_i)$; $h_j^y \equiv (y_{j+1} - y_j)$) and define nodal averaged fluxes in the X and Y directions:

$$\bar{\phi}_{gx}(x) \equiv \frac{1}{h_j^{(y)}}\int_{y_j}^{y_{j+1}}\phi_g(x,y)\,dy$$

$$\bar{\phi}_{gy}(y) \equiv \frac{1}{h_i^{(x)}}\int_{x_i}^{x_{i+1}}\phi_g(x,y)\,dx \qquad (1.87)$$

Comparison with the two-dimensional analog of (1.86) shows that

$$\frac{1}{h_i^{(x)}} \int_{x_i}^{x_{i+1}} \phi_{g_x}(x)dx = \frac{1}{h_j^{(y)}} \int_{y_i}^{y_{i+1}} \phi_{gy}(y)dy = \bar{\phi}_g^{(ij)}$$

To obtain an equation for the $\bar{\phi}_{gx}$ we integrate the basic group diffusion equation for the node (1.28) over $h_j^{(y)}$ at a particular value of x within $h_i^{(x)}$.

$$- D_g^{(ij)} \frac{d^2\phi_{gx}^{(x)}}{dx^2} + L_{gy(x)}^{(ij)} + \Sigma_{tg}^{(ij)} \bar{\phi}_{gx}(x)$$

$$= \sum_{g'=1}^{G} \left[\Sigma_{gg'}^{(ij)} + \chi_g \nu \Sigma_{fg'}^{(ij)} \right] \bar{\phi}_{jx}(x)$$

$$g = 1, 2, \ldots G \qquad (1.88)$$

the transverse leakage term $L_{gy}^{(ij)}$ being defined as

$$L_{gy}^{(ij)}(x) \equiv - D_g^{(ij)} \frac{1}{h_j^{(y)}} \left[\frac{\partial}{\partial y} \phi_g(x, y_{j+1}) - \frac{\partial}{\partial y} \phi_g(x, y_j) \right] \qquad (1.89)$$

By integrating (1.28) over $h_i^{(x)}$ at a particular y, an analogous equation for $\bar{\phi}_{gy}(y)$ can be obtained. In this equation transverse leakage terms in the X-direction appear ($L_{gx}^{(ij)}(y)$).

If the transverse leakages $L_{gy}^{(ij)}(x)$ were known, it could be possible to solve for the $\bar{\phi}_{gx}(x)$ within node (ij) in terms of $\bar{\phi}_{gx}(x_i)$ and $-D_g^{ij} \frac{d\phi_{gx}(x_i)}{dx}$ at the interface between node (ij) and node (i-1, j), and then by integrating over $h_i^{(x)}$, $\bar{\phi}_g^{(ij)}$ could be relaced to these two quantities. The $\bar{\phi}_g^{(i-1,j)}$ (average group flux in node (i-1, j)) could also be found in terms of these same two quantities by a similar procedure carried out for node (i-1, j) and taking advantage of the continuity of flux and current across the nodal interface. Thus if the $L_{gy}^{(ij)}(x)$ and $L_{gy}^{(i-1,j)}(x)$ were zero it would be possible to obtain two relationships of the form

$$\bar{\phi}_g^{(ij)} = f_1(\bar{\phi}_{gx}(x_i), - D_g^{(ij)} \frac{d\bar{\phi}_{gx}(x_i+)}{dx})$$

$$\bar{\phi}_g^{(i-1,j)} = f_2(\bar{\phi}_{gx}(x_i), - D_g^{(i-1,j)} \frac{d\bar{\phi}_{gx}(x_i-)}{dx}) \qquad (1.90)$$

Then by eliminating $\bar{\phi}_{gx}(x_i)$ from these two equations we could derive a relationship of the form

$$\bar{J}_{gx}(x_i) \equiv - D_g^{(ij)} \frac{d\phi_{gx}(x_i+)}{dx} = - D_g^{(i-1,j)} \frac{d\phi_{gx}(x_i-)}{dx}$$

$$= f_3(\bar{\phi}_g^{(ij)}, \bar{\phi}_g^{(i-1,j)}) \qquad (1.91)$$

For the case at hand the basic nodal equation (1.85) becomes

$$\frac{1}{h_i^{(x)} h_j^{(y)}} \left[h_j^{(y)} (\bar{J}_{gx}(x_i) - \bar{J}_{gx}(x_{i-1}) + h_i^{(x)} (\bar{J}_{gy}(y_j) - \bar{J}_{gy}(y_{j-1}) \right]$$

$$+ \Sigma_{tg}^{(ij)} \bar{\phi}_g^{(ij)} = \sum_{g'=1}^{G} \Sigma_{gg'}^{(ij)} + \chi_g \nu \Sigma_{fg}^{(ij)} \quad \bar{\phi}_{g'}^{(ij)} \tag{1.92}$$

Hence by using (1.91) to eliminate $\bar{J}_g(x_i)$ and expressions analogous to (1.91) to eliminate the other three leakage terms we could convert (1.92) into a "five-point difference equation" relating $\bar{\phi}_g^{(ij)}$ and its four nearest neighbors. Standard finite difference procedures could then be used to solve for the $\bar{\phi}_g^{(ij)}$.

All this is rigorously possible only if the transverse leakage terms in the Y-directions are neglected in the manipulations leading to the transverse leakage formula (1.91) for the X-direction. In fact, however, such neglect leads to error, so that someway of dealing with the term $L_{gy}^{(ij)}(x)$ in (1.88) must be concocted. The simplest procedure is to replace $\phi_g(x,y_{j+1})$ and $\phi_g(x,y_j)$ in (1.89) by their average values $\bar{\phi}_{gy}(y_{j+1-})$ and $\bar{\phi}_{gy}(y_{j+})$. Eq. (1.89) then becomes

$$L_{gy}^{(ij)}(x) \approx \bar{J}_{gy}(y_{j+1}) - \bar{J}_{gy}(y_j) \equiv \bar{L}_{gy}^{(ij)} \tag{1.93}$$

The solution of (1.88) leading to (1.91) must then be carried out with this (constant) value of $L_{gy}^{(ij)}$ treated as an inhomogeneous source term. Thus the following iteration scheme is suggested:

1) Solve (1.88) and determine (1.91) with $L_{gy}^{(ij)}(x) = 0$.

2) Substitute (1.91) and analogous expressions for the three other average currents into (1.92) and solve the resulting 5-point equations.

3) With the values of $\bar{\phi}_g^{(ij)}$ so obtained evaluate the $\bar{J}_{gx}(x_i)$'s etc. using (1.91).

4) Use these to form the inhomogeneous term $\bar{L}_{gy}^{(ij)}$ in (1.88); solve that equation and continue the iteration procedure.

An improved way of dealing with the $L_{gy}^{(ij)}(x)$ etc. has been suggested by Finnemann [19]. This is to fit $L_{gy}^{(ij)}(x)$ to a quadratic polynomial over the three-node range $x_{i-1} \le x \le x_{i+2}$ expressing the coefficients of the polynomial in terms of the average transverse leakages $\bar{L}_{gy}^{(i-1,j)}$, $\bar{L}_{gy}^{(ij)}$ and $\bar{L}_{gy}^{(i+1,j)}$. The resulting quadratic function is then used to approximate the x-dependence of $L_{gy}^{(ij)}(x)$ in (1.88) in the range $x_i \le x \le x_{i+1}$. As before, the transverse leakages needed to generate polynomials are formed, using (1.91), from the previous iterate for the $\bar{\phi}_g^{(ij)}$.

The problem of solving (1.91) can be solved in a number of ways. It can be done analytically [18] or by expanding the

X-dependence of the $\bar{\Phi}_{gx}(x)$ in polynomials, determining some of the coefficients by applying continuity and boundary conditions and determining the rest by weighted residual procedures. These polynomial schemes can be carried out for a whole row of nodes at once [16] or one node at a time [17,18]. In the latter case it is convenient to express the polynomials in terms of partial currents (1.70) across the nodal surfaces rather than the flux and total current values on those surfaces.

Very encouraging results have been obtained with the new nodal methods. For a given degree of accuracy they are one or two orders of magnitude faster than finite difference methods. They have been extended to time-dependent problems and to situations in which the nodal group-parameters are mildly space dependent (such as will occur if fuel depletion is not uniform over the node). Approximate values of local power peaks can be recovered from the nodal fluxs and surface currents generated in the course of carrying out a solution. The major concerns about them are that (to date) they deal only with Cartesian geometries and they cannot be applied directly to reactors composed of drastically heterogeneous nodes (such as the nodes containing cross-shaped rods in a BWR). The latter problem can be overcome by the use of nodal-homogenized group parameters as explained earlier. Provided this is done accurately, the nodal schemes appear to be a very powerful tool for the analysis of light water reactors.

1.5 Extension of Static Criticality Calculations to Fuel Depletion Problems

The extension of criticality calculations to depletion is straight forward but greatly increases the costs of calculations unless it is carried out carefully.

At first the extension appears to raise major mathematical problems. Depletion is a time-dependent phenomenon, the result of which is to change local concentrations of fuel and introduce fission products so that local group parameters change with time in a way that depends on the local group fluxes. Moreover, significant depletion takes place only in reactors operating at high power. Thus local temperatures and densities may vary in a manner that depends on the local fluxes and depleting fuel concentrations. But the fluxes themselves also depend on the local temperatures and densities. Thus at first it would appear necessary to deal with non-linear, time dependent sets of equations describing the depletion, heat transfer of phenomena and the neutron flux behavior simultaneously.

In practice the situation is not nearly that bad. Depletion effects are so slow that steady state neutron and heat transfer equations can be used. Also, the depletion calculations can be done separately from the nuclear-thermal calculations.

Thus the initial flux shape is assumed to remain constant during the first depletion time step; then, with the newest material concentrations, group parameters are up-dated and a new flux shape is determined. This latest shape is the one used for the

next time step. Thus the depletion and nuclear-thermal calculations are done in tandom and as far as depletion is concerned the nuclear calculations are standard static, linear computations.

The thermal-hydraulic computations do complicate matters. But this is a complication encountered whenever the temperature and density distributions throughout a reactor affect flux shapes. It is necessary to iterate between temperature density distribution and flux distribution until the steady state temperature density profile associated with a particular flux shape is consistent with the flux shape associated with that temperature-density profile. A consistent equilibrium xenon concentration, control rod position or soluble poison concentration leading to criticality must also be found by iterative procedures. The startegy for this type of iteration is to try first to converge the quantities that produce the greatest effects. Thus, if the flux shape is quite sensitive to control rod bank position but the control rod bank position is not very sensitive to the temperature-density distribution (and hence to the flux shape), first find the control rod bank position corresponding closely to criticality but to a possibly incorrect temperature-density profile. Then improve the temperature-density profile. Such iterative searches are complicated. However, as previously noted, they are a consequence of the reactor's being at power rather than of depletion.

The real problems associated with depletion are the need to determine changes in group-parameters due to depletion at all mesh points in fuel regions for a large segment of the reactor (symmetry usually permits dealing with only a quarter or an eighth of the core) and the consequent amount of data that must be handled. Thus, if it is necessary to keep track of say 15 isotopic densities (U^{235}, U^{236}, Pu^{239}, Pu^{240}, Pu^{241}, B^{10}, several fission products, etc.), at 100,000 mesh points comprising the fuel region for an eighth of the core, 1.5 million concentrations must be stored, 100,000 spectrum calculations must be run and $\sim$ 400,000xG group-parameters must be reconstructed each depletion time step.

Two simplifying approximations are generally made to overcome these difficulties. The first is called block depletion and consists simply in using the <u>average</u> fluxes throughout nodal regions rather than the point fluxes to do the depletion calculations. If nodal regions each containing, say, 100 mesh cubes are selected the amount of data to be stored and the amount of calculational work is cut by a factor of 100.

The second simplifying procedure used to make depletion calculations manageable is to determine changes in group parameters by constructing them from what are called "fitted microscopic cross sections". The idea is based on the observation that at any time, t, in the course of reactor depletion a group parameter, say, $\Sigma_{ag}(\underline{r},t)$ can be expressed as

$$\Sigma_{ag}(\underline{r},t) = \sum_j n^j(\underline{r},t)\ \sigma^j_{ag}(\underline{r},t) \qquad (1.94)$$

where $n^j(\underline{r},t)$ is the concentration of isotope-j at point $\underline{r}$

and time t and $\sigma_{ag}^{j}(\underline{r},t)$ is the microscopic group-g absorption cross section for isotope-j at that point and time. The concentrations $n^{j}(\underline{r},t)$ change in time because of the depletion processes. The microscopic group-cross-sections also change since the local neutron spectrum itself depends on local isotopic concentrations and hence on time. (See the discussion relevant to Eq. 1.17 through (1.24.) In the fitted constants procedure we try to estimate in advance how the local spectrum will change as depletion proceeds. To do that we perform what are called "point depletion" calculations for each different fuel composition making up the initial loading of the reactor. (Generally there are only 3 or 4 such initial compositions.) To do a "point depletion" we start with the initial concentrations of the fuel composition and compute few group parameters in the usual way. Then with $\nabla^2\phi_g$ set equal to $-B_m^2\phi_g$ where B_m^2 is the materials buckling we deplete the composition for a depletion time step (~ 1000 hours). A new spectrum calculation is then performed, new few group parameters are determined and another depletion step is taken. Since microscopic group parameters corresponding to the up-dated spectra can be obtained at each time step, we can form a table of such quantities as σ_{ag}^{j} vs. some parameter (such as the total fission energy released) that characterizes the degree of depletion. Then as the whole core depletion proceeds we can generate the σ_{ag}^{j} for that fuel composition at any time and location just by keeping track of how much energy has been released at that location. Thus pointwise values of $\Sigma_{ag}(\underline{r},t)$ (Eq. 1.94) can be found as needed, and the need to perform a spectrum calculation at each mesh point or nodal block at every time step is reduced to that of doing one for each initial composition. The saving is great since there may be 1000 nodal blocks but only 4 initial fuel compositions. The error in the procedure is due to replacing the $\nabla^2\phi_g$ at points by $B_m^2\phi_g$. This error is usually small. Note that the n^j in (1.94) used with fitted the values σ_{ag}^{j} are those obtained from the full core, space dependent depletion. The "point depletions" are done only to generate the σ_{ag}^{j}.

With the block depletion and fitted constants procedures (along with a few more minor approximations described in Ref. (3) Chapter 6) the mechanical problems of data handling associated with reactor depletion become quite tractable, and depletion calculations are reduced to a manageable sequence of steady state criticality computations.

2. Reactor Kinetics

In discussing the mathematical models used to describe transients in nuclear reactors and the techniques used to solve the relevant equations we shall assume a general familiarity with the physical picture that underlies the kinetic behavior of a reactor (large neutron population, very fast neutron speeds, delayed neutron precursors and their relatively slow decay periods, reactor parameters that are time dependent because of temperature and density feedback phenomena). We shall also assume a qualitative understanding of such terms as subcritical, supercritical, prompt critical, reactor period, scram, runaway, etc. With a general familiarity with such

concepts and terms assumed we shall then begin with a discussion of the time dependent group diffusion equations and methods for solving them and follow that by a derivation of the point kinetics equations along with discussion of tne kinetics parameters and the measurement of reactivity. Finally, we shall indicate how feedback effects are accounted for.

2.1 Space Dependent Kinetics Equations

a) The Time Dependent Group Diffusion Equations

We shall use the group diffusion model to describe space dependent kinetics effects. Thus it will be necessary to extend (1.28) to the time dependent ca.e. This is a straightforward procedure: We first note that, if the creation rate of neutrons exceeds the destruction rate, the number of group-g neutrons $(\frac{1}{v_g}\phi_g)$ will increase at a rate $\frac{\partial}{\partial t}(\frac{\phi_g}{v_g})$ (v_g is the average speed of neutrons belonging to group-g). It is also necessary to distinguish between prompt neutrons appearing directly as the result of a fission and delayed neutrons appearing as the result of the decay of a precursor. With these matters accounted for and $C_i(\underline{r},t)$, β_i^j and λ_i standing for the local concentration of the i^{th} precursor group, the fraction of the neutrons from a fission of isotope j that eventually appear from the decay of precursor i, and λ_i the radioactive decay constant of precursor group-i, Equation (1.28) extended to the time dependent case becomes

$$\frac{\partial}{\partial t}\left(\frac{\phi_g(\underline{r},t)}{v_g}\right) = \sum_{g'=1}^{G}\left[\Sigma_{gg'}(\underline{r},t) + \sum_j(1-\beta^j)\chi_{pg}^j\nu\Sigma_{fg'}^j(\underline{r},t)\right]\phi_{g'}$$

$$+ \sum_{i=1}^{I}\chi_{ig}\lambda_i C_i(\underline{r},t) + \nabla\cdot D_g(\underline{r},t)\nabla\phi_g(\underline{r},t) - \Sigma_{tg}(\underline{r},t)\phi_g(\underline{r},t)\ ;$$

$$g = 1, 2, \ldots G \qquad (2.1)$$

where $\beta^j \equiv \sum_i \beta_i^j$; χ_{pg}^j is the fraction of prompt neutrons appearing in group-g from fission of isotope-j, and χ_{ig} is the fraction of delayed neutrons emitted by decay of precursor-i that appear in group-g. (Note that we have now accounted explicitly for fissioning of a number of isotopes, j.) To complete (2.1) we need equations specifying the rate of change of the $C_i(\underline{r},t)$. These are

$$\frac{\partial C_i(\underline{r},t)}{\partial t} = \sum_j\beta_i^j\sum_{g=1}^{G}\nu\Sigma_{fg'}^j(\underline{r},t)\phi_{g'}(\underline{r},t) - \lambda_i C_i(\underline{r},t); \qquad (2.2)$$

$$i = 1, 2, \ldots I$$

Eq. (2.1) states mathematically that the rate of change of the number of group-g neutrons per cc per second equals the difference between the creation and loss rate of such neutrons (a neutron can be "lost" from the unit volume about point $\underline{r}$ and the energy group-g by leakage and scattering as well as by absorption.) Eq. 2.2 makes an analogous statement about the concentration of the i^{th} precursor group. Note that all the group parameters are shown to be functions of time. We shall not discuss at this time how such time dependence is accounted for mathematically. (See Section 2.3 below.)

b) Finite Difference Solutions of the Group Diffusion Equations

With Eqs. (2.1) and (2.2) taken as a basic numerical model for the description of transient neutron behavior we shall first indicate the matrix form which results when the spatial parts of these equations are written in finite difference form. Then we shall discuss methods for solving the time dependent matrix equations that result. Only the simplest one-neutron group, one-precursor-group, homogeneous slab geometry will be shown in finite difference form explicitly. Generalizations of the relevant matrices that result when more groups and more dimensions are accounted for will merely be described qualitatively.

In finite difference form, for a homogeneous slab reactor, the one-group time-dependent diffusion equation with one group of delayed precursors is (see Eq. (1.34) and (1.46)

$$\frac{D}{h^2}(\phi_{j+1}+\phi_{j-1}-2\phi_j) + (\nu\Sigma_f(1-\beta)-\Sigma_a)\phi_j+\lambda C_j = \frac{1}{v}\dot{\phi}_j \qquad (2.3)$$

$$\beta\nu\Sigma_f\phi_j - \lambda C_j = \dot{C}_j$$

where subscript j refers to mesh points (not precursor groups).

In matrix from Eq. (2.3 becomes

$$\begin{bmatrix} a & \frac{Dv}{h^2} & 0 & \lambda v & 0 \\ \frac{Dv}{h^2} & a & \frac{Dv}{h^2} & 0 & \lambda v \\ 0 & \frac{Dv}{h^2} & a & & \\ \beta\nu\Sigma_f & 0 & & -\lambda & 0 \\ 0 & \beta\nu\Sigma_f & & 0 & -\lambda \end{bmatrix} \begin{bmatrix} \phi_1 \\ \phi_2 \\ \phi_{N-1} \\ C_1 \\ C_2 \\ C_{N-1} \end{bmatrix} = \frac{d}{dt} \begin{bmatrix} \phi_1 \\ \phi_2 \\ \phi_{N-1} \\ C_1 \\ C_2 \\ C_{N-1} \end{bmatrix} \qquad (2.4)$$

where

$$a \equiv \nu\Sigma_f(1-\beta)v - (\Sigma_a + \frac{2D}{h^2})\, v \qquad (2.5)$$

In abbreviated form Eq. (2.4) may be written

$$\underline{\underline{B}}\ \underline{\psi} = \dot{\underline{\psi}} \qquad (2.6)$$

or

$$\begin{pmatrix} \underline{\underline{B}}_{11} & \underline{\underline{B}}_{12} \\ \underline{\underline{B}}_{21} & \underline{\underline{B}}_{22} \end{pmatrix} \begin{pmatrix} \underline{\phi} \\ \underline{C} \end{pmatrix} = \frac{d}{dt} \begin{pmatrix} \underline{\phi} \\ \underline{C} \end{pmatrix} \qquad (2.7)$$

where $\underline{\underline{B}}_{11}$ is the tridiagonal part of $\underline{\underline{B}}$ and $\underline{\underline{B}}_{12}$, $\underline{\underline{B}}_{21}$ and $\underline{\underline{B}}_{22}$ are diagonal. (Note that $\underline{\underline{B}}_{11}$ and $\underline{\underline{B}}_{21}$ are in general time-dependent.)

For more general models (more than one neutron or precursor group, more than one dimension, heterogeneous reactor structures with non-uniform mesh structure) the matrix equations analogous to (2.4) become larger. But they still have the same general structure.

Thus if 6 delayed precursor groups are included, 5 additional matrices of the type $\underline{\underline{B}}_{12}$ (i.e. diagonal) are added to the first row of the supermatrix $\underline{\underline{B}}$, 5 additional matrices of the form $\underline{\underline{B}}_{21}$ are added to the first column, and 5 of the form $\underline{\underline{B}}_{22}$ are added to the diagonal. Thus (2.7) becomes

$$\begin{pmatrix} B_{11} & B_{12} & B_{13} & \cdots & B_{16} \\ B_{21} & B_{22} & 0 & & 0 \\ B_{31} & 0 & B_{33} & & 0 \\ \vdots & & \vdots & & \vdots \\ B_{61} & 0 & 0 & \cdots & B_{66} \end{pmatrix} \begin{pmatrix} \phi \\ C_1 \\ C_2 \\ \\ C_6 \end{pmatrix} = \frac{d}{dt} \begin{pmatrix} \phi \\ C_1 \\ C_2 \\ \\ C_6 \end{pmatrix} \qquad (2.8)$$

where the elements of the column vectors $\underline{C}_i$ are the concentrations of group-i delayed precursors at the internal mesh points.

For two dimensional cases the submatrix $\underline{\underline{B}}_{11}$ has 5 stripes rather than 3; for three dimensions it has 7 stripes.

For more than one group, the submatrix $\underline{\underline{B}}_{11}$ becomes more general. If $\phi_{ijk}^{(g)}$ refers to the group-g flux at mesh point (i,j,k) and the elements of the column vector ϕ are clustered by points

$$(\underline{\phi} = \mathrm{Col}\{\phi_{111}^{(1)}, \phi_{111}^{(2)}, \ldots, \phi_{111}^{(G)}, \phi_{211}^{(1)}, \phi_{211}^{(2)}, \ldots, \phi_{211}^{(G)}, \ldots\}),$$

then $\underline{\underline{B}}_{11}$ becomes 7-stripe with each element a full G x G matrix. If, on the other hand, the elements of ϕ are clustered one group at a time

$$(\underline{\phi} = \mathrm{Col}\{\phi_{111}^{(1)}, \phi_{211}^{(1)}, \phi_{311}^{(1)}, \ldots, \phi_{IJK}^{(1)}, \phi_{111}^{(2)}, \ldots, \phi_{I,J,K}^{(G)}\}),$$

additional submatrices having the same form as $\underline{\underline{B}}_{11}$ (i.e. 7-stripe) appear along the diagonal of $\underline{\underline{B}}$, there being one such additional submatrix for each additional group. In addition, surrounding the blocks along the diagonal of $\underline{\underline{B}}$, there appear diagonal submatrices specifying the transfer of neutrons from one group to another.

(i) Implicit Methods of Solution[20,21,22]

One standard procedure for solving the time dependent group diffusion equations is to integrate Eq. (2.7) - or a more general version - over a time interval Δ:

$$\begin{pmatrix} \underline{\phi}^{(n+1)} \\ \underline{C}^{(n+1)} \end{pmatrix} - \begin{pmatrix} \underline{\phi}^{(n)} \\ \underline{C}^{(n)} \end{pmatrix} = \int_0^{\Delta} \begin{pmatrix} \underline{\underline{B}}_{11}(\tau) & \underline{\underline{B}}_{12} \\ \underline{\underline{B}}_{21}(\tau) & \underline{\underline{B}}_{22} \end{pmatrix} \begin{pmatrix} \phi(\tau) \\ \underline{C}(\tau) \end{pmatrix} d\tau \quad \cong$$

$$\cong \Delta \begin{pmatrix} \underline{\underline{B}}_{11}^{(n+1)} & \underline{\underline{B}}_{12} \\ \underline{\underline{B}}_{21}^{(n+1)} & \underline{\underline{B}}_{22} \end{pmatrix} \begin{pmatrix} \underline{\underline{\theta}}_p & 0 \\ 0 & \underline{\underline{\theta}}_d \end{pmatrix} \begin{pmatrix} \underline{\phi}^{(n+1)} \\ \underline{C}^{(n+1)} \end{pmatrix} +$$

$$+ \Delta \begin{pmatrix} \underline{\underline{B}}_{11}^{(n)} & \underline{\underline{B}}_{12} \\ \underline{\underline{B}}_{21}^{(n)} & \underline{\underline{B}}_{22} \end{pmatrix} \begin{pmatrix} \underline{\underline{I}}-\underline{\underline{\theta}}_p & 0 \\ 0 & I-\theta_d \end{pmatrix} \begin{pmatrix} \underline{\phi}^{(n)} \\ \underline{C}^{(n)} \end{pmatrix} \qquad (2.9)$$

where $\underline{\underline{\theta}}_p$ and $\underline{\underline{\theta}}_d$ are diagonal matrices of numbers between 0 and 1. All the elements of $\underline{\underline{\theta}}_p$ are the same and all the elements of $\underline{\underline{\theta}}_d$ are the same but not necessarily equal to those of $\underline{\underline{\theta}}_p$. The aim is to choose the θ's so that the integral in (2.9) is closely approximated by some average of the values of the integrand at the beginning and end of the time step.

To solve (2.9), it is convenient to eliminate $\underline{C}^{(n+1)}$. To do so, we write out (2.8) as

$$\frac{1}{\Delta}\{ \underline{\phi}^{(n+1)} - \underline{\phi}^{(n)} \} = \underline{\underline{B}}_{11}^{(n+1)} \underline{\underline{\theta}}_p \underline{\phi}^{(n+1)} + \underline{\underline{B}}_{12} \underline{\underline{\theta}}_d \underline{C}^{(n+1)} +$$

$$+ \underline{\underline{B}}_{11}^{(n)} \left(\underline{\underline{I}}-\underline{\underline{\theta}}_p\right) \underline{\phi}^{(n)} + \underline{\underline{B}}_{12} \left(\underline{\underline{I}}-\underline{\underline{\theta}}_d\right) \underline{C}^{(n)}$$

and

$$\frac{1}{\Delta}\{ \underline{C}^{(n+1)} - \underline{C}^{(n)} \} = \underline{\underline{B}}_{21}^{(n+1)} \underline{\underline{\theta}}_p \underline{\phi}^{(n+1)} + \underline{\underline{B}}_{22} \underline{\underline{\theta}}_d \underline{C}^{(n+1)} +$$

$$+ \underline{\underline{B}}_{21}^{(n)} \left(\underline{\underline{I}}-\underline{\underline{\theta}}_p\right) \underline{\phi}^{(n)} + \underline{\underline{B}}_{22} \left(\underline{\underline{I}}-\underline{\underline{\theta}}_d\right) \underline{C}^{(n)} \qquad (2.10)$$

or

$$\underline{\phi}^{(n+1)} = \left(\underline{\underline{I}}-\Delta \underline{\underline{B}}_{11}^{(n+1)} \underline{\underline{\theta}}_p\right)^{-1} \{ \underline{\underline{I}}+\Delta \underline{\underline{B}}_{11}^{(n)} (\underline{\underline{I}}-\underline{\underline{\theta}}_p) \underline{\phi}^{(n)} +$$

$$+ \Delta \underline{\underline{B}}_{12} \underline{\underline{\theta}}_d \underline{C}^{(n+1)} + \Delta \underline{\underline{B}}_{12} (\underline{\underline{I}}-\underline{\underline{\theta}}_d) \underline{C}^{(n)} \}$$

and

$$\underline{C}^{(n+1)} = \left(\underline{\underline{I}}-\Delta \underline{\underline{B}}_{22} \underline{\underline{\theta}}_d\right)^{-1} \{ \underline{\underline{I}}+\Delta \underline{\underline{B}}_{22} (\underline{\underline{I}}-\underline{\underline{\theta}}_d) \underline{C}^{(n)} +$$

$$+ \Delta \underline{\underline{B}}_{21}^{(n+1)} \theta_p \underline{\phi}^{(n+1)} + \Delta \underline{\underline{B}}_{21}^{(n)} (\underline{\underline{I}}-\underline{\underline{\theta}}_p) \phi^{(n)} \} \qquad (2.11)$$

If now we use the second of Eq. (2.11) to eliminate $\underline{C}^{(n+1)}$ from the first equation, we obtain

$$\underline{\phi}^{(n+1)} = \left[\underline{I}-\Delta\underline{B}_{11}^{(n+1)}\underline{\theta}_p - \Delta\underline{B}_{12}\underline{\theta}_d(I-\Delta\underline{B}_{22}\underline{\theta}_d)^{-1}\,\Delta\underline{B}_{21}^{(n+1)}\underline{\theta}_p\right]^{-1}\underline{S}^{(n)}$$

$$\equiv \underline{M}^{-1}\,\underline{S}^{(n)} \qquad (2.12)$$

where $\underline{S}^{(n)}$ is a column vector involving only $\underline{\phi}^{(n)}$ and $\underline{C}^{(n)}$ and all terms in the inverse are diagonal except $\underline{B}_{11}^{(n+1)}$. Thus the inverse $\underline{M}^{-1}$ is no more difficult to take than $\left[\underline{I}-\Delta\underline{B}_{11}^{(n+1)}\underline{\theta}_p\right]^{-1}$. More important than that is the fact it is only half the size of $\left[\underline{I}-\Delta\underline{B}\underline{\theta}\right]^{-1}$, the matrix we would encounter if we tried to solve (2.9) directly for $(\underline{\phi}^{(n+1)}, \underline{C}^{(n+1)})$. Finally, if 6 delayed precursor groups are considered (Eq. 2.8) an equation of the form (2.12) can again be derived, the third term in the inverse being replaced by a sum over 6 diagonal matrices so that, again, taking the inverse $\underline{M}^{-1}$ is no more complicated than taking the inverse $\left[\underline{I} - \Delta\underline{B}_{11}^{(n+1)}\underline{\theta}_p\right]^{-1}$.

Finding $\underline{\phi}^{(n+1)}$ thus reduces to the problem of finding the inverse of a 3, 5 or 7-stripe matrix depending on whether the problem is in one, two or three dimensions.

This is a problem we have already discussed for the static finite difference equations. (See Eqs. 1.45 - 1.55.) For the one dimensional case the forward elimination-backward substitution method is used (generally with $\underline{\phi}^{(n)}$ so arranged that $\underline{B}_{11}^{(n)}$ is a tridiagonal matrix each element being G x G). For two and three dimensions $\underline{B}_{11}^{(n)}$ is split into a lower and upper triangular part and an iterative procedure is used (generally one group at a time).

ii) Alternating Direction Methods (23, 24)

Whether done directly (possible with 3-stripe matrices) or iteratively (5 or 7-stripe matrices) the solutions (2.12) we have been discussing yield $\phi^{(n+1)} = M^{-1}S^{(n)}$; that is, the inverse of the full matrix M is in effect found. There is an alternate class of solution methods for Eq. (2.6) called alternating direction methods that permit a solution of (2.6) to be found for two and three dimensions by a non-iterative method.

As developed, these deal with the spacially differenced diffusion equations in the form (2.6) (rather than (2.7)). Further, it is assumed that $\underline{B}$ has some constant, average value during two successive time steps. With these assumptions the essential step in an alternating direction method is to split the matrix $\underline{B}$ into a sum $\underline{B}_1 + \underline{B}_2$ such that, while $\underline{I}-\underline{B}$ is not directly invertable, $\underline{I}-\underline{B}_1$ and $\underline{I}-\underline{B}_2$ are. Specifically we time-difference Eq. (2.6) as

$$\frac{1}{\Delta}\{\underline{\psi}^{(n+1)} - \underline{\psi}^{(n)}\} = \underline{B}_2\,\underline{\psi}^{(n+1)} + \underline{B}_1\,\underline{\psi}^{(n)}$$

$$\frac{1}{\Delta}\{\underline{\psi}^{(n+2)} - \underline{\psi}^{(n+1)}\} = \underline{B}_1\,\underline{\psi}^{(n+2)} + \underline{B}_2\,\underline{\psi}^{(n+1)} \qquad (2.13)$$

so that

$$\underline{\psi}^{(n+2)} = \left[\underline{I}-\Delta\underline{B}_1\right]^{-1}\left[\underline{I}+\Delta\underline{B}_2\right]\left[\underline{I}-\Delta\underline{B}_2\right]^{-1}\left[\underline{I}+\Delta\underline{B}_1\right]\underline{\psi}^{(n)} \qquad (2.14)$$

It might appear that reversing the order of the operations in the second of Eqs. (2.13) is a needless complexity. However, this is not the case. Unless the reversal is carried out the method is numerically unstable. It should also be noted that the splitting in the second equation (2.13) need not be in the same as in the first. We shall not, however, discuss this in greater generality. In face we shall restrict further discussion to the one-group case (Eq. (2.8)) in two dimensions.

We consider three ways of splitting $\underline{\underline{B}}$ so that the inverses indicated in (2.14) can be found readily.

(1) Alternating Direction Implicit

Here we let $\underline{\underline{B}}_1$ be 1/2 the diagonal of $\underline{\underline{B}}$, plus all the submatrices $\underline{\underline{B}}_{ij}$ $j > i$ in the upper triangular portion of $\underline{\underline{B}}$ plus that portion of the off-diagonal parts of $\underline{\underline{B}}_{11}$ associated with diffusion in one of the two directions. The remainder of $\underline{\underline{B}}$ then consists of 1/2 the diagonal, plus all the $\underline{\underline{B}}_{ij}$ $i > j$ below the diagonal, plus the off-diagonal part of $\underline{\underline{B}}_{11}$ associated with diffusion in the second of the two directions. With this splitting, taking the inverse of both $\underline{\underline{I}}-\Delta\underline{\underline{B}}_1$ and $\underline{\underline{I}}-\Delta\underline{\underline{B}}_2$ is like solving a sequence of one-dimensional problems in which $\underline{\underline{B}}_{11}$ is 3-stripe. We have already seen that this can be done by the forward-elimination-backward-substitution method. Thus finding $\underline{\psi}^{(n+1)}$ by (2.14) is a direct, non-iterative procedure.

(2) Alternating Direction Explicit

In this approach we take $\underline{\underline{B}}_1$ to be 1/2 the diagonal part of $\underline{\underline{B}}$ and all the rest of $\underline{\underline{B}}$ lying above the diagonal. Hence $\underline{\underline{B}}_2$ is 1/2 of the diagonal and all the lower triangular part of $\underline{\underline{B}}$. Then operation of the inverse $\left[\underline{\underline{I}}+\Delta\underline{\underline{B}}_2\right]^{-1}$ on $\underline{\underline{I}}+\Delta\underline{\underline{B}}_1\ \underline{\psi}^{(n)}$ in Eq. (2.14) can be found by a straightforward extension of (1.52). The operation of $\left[\underline{\underline{I}}-\Delta\underline{\underline{B}}_1\right]^{-1}$ on $\left[\underline{\underline{I}}+\Delta\underline{\underline{B}}_2\right]\left[\underline{\underline{I}}-\Delta\underline{\underline{B}}_2\right]^{-1}\left[\underline{\underline{I}}+\Delta\underline{\underline{B}}_1\right]\underline{\psi}^{(n)}$ is found by an extension of (2.1.53). Note that the first inverse is taken starting with the first element of the column vector $\left[\underline{\underline{I}}+\Delta\underline{\underline{B}}_1\right]\underline{\psi}^{(n)}$ and the second with the last element of $\left[\underline{\underline{I}}+\Delta\underline{\underline{B}}_2\right]\left[\underline{\underline{I}}-\Delta\underline{\underline{B}}_2\right]^{-1}\left[\underline{\underline{I}}+\Delta\underline{\underline{B}}_1\right]\underline{\psi}^{(n)}$.

(3) The Checkerboard Scheme

In both the splitting schemes just described there is a certain lack of symmetry in the way the flux precursor values are advanced in time. In the implicit method new values at mesh points on a given line are found using older values on adjacent lines. In the explicit method the new value at a point is found using two neighboring values just found during the present mesh sweep and two others found on a previous sweep of the mesh in the opposite direction.

An alternate splitting that appears to be more symmetric is one that advances in time all the x-points in Figure (7)

x o x o x o x
o x o x o x o
x o x o x o x
o x o x o x o

Fig. 7: The Checkerboard Splitting

or all the o-points as a block. To develop such a splitting we define a block diagonal matrix $\underline{\underline{I}}_x$, each block being a diagonal

N x N matrix (N being the total number of internal mesh points) and the number of blocks being equal to the sum of the number of neutron plus precursor groups. The elements of $\underline{\underline{I}}_x$ are 0 or 1 and are chosen so that the column vector $\underline{\underline{I}}_x \underline{\psi}$ contains all and only the fluxes and precursor concentrations at the X-points. A corresponding vector $\underline{\underline{I}}_o \equiv \underline{\underline{I}} - \underline{\underline{I}}_x$ is such that $\underline{\underline{I}}_o \underline{\psi}$ contains all and only the fluxes and precursor concentrations at the o-points.

We then difference Eq. (2.6) in two stages to get an expression for $\underline{\psi}^{(n+2)}$ in terms of $\underline{\psi}^{(n)}$. Each stage is accomplished in two steps. The overall procedure is as follows:

Stage 1, Step 1:

Integrate Eq. (2.6) by the explicit method

$$\underline{\psi}^{(n+1)} - \underline{\psi}^{(n)} = \Delta \underline{\underline{B}} \underline{\psi}^{(n)} \tag{2.15}$$

but do so only for the X-points so that

$$\underline{\underline{I}}_x \underline{\psi}^{(n+1)} = \underline{\underline{I}}_x \left[\underline{\underline{I}}+\Delta\underline{\underline{B}}\right] \underline{\psi}^{(n)} \tag{2.16}$$

This procedure is straightforward, no inverses at all are required.

Stage 1, Step 2:

Integrate Eq. (2.6) implicitly for the o-points

$$\underline{\underline{I}}_o \{ \underline{\psi}^{(n+1)} - \underline{\psi}^{(n)} \} = \Delta \underline{\underline{I}}_o \underline{\underline{B}} \underline{\psi}^{(n+1)} \tag{2.17}$$

and on the right hand side take $\underline{\psi}^{(n+1)}$ to be $\underline{\underline{I}}_o \underline{\psi}^{(n+1)} + \underline{\underline{I}}_x \underline{\psi}^{(n+1)}$ with $\underline{\underline{I}}_x \underline{\psi}^{(n+1)}$ given by (2.16). We then get

$$\underline{\underline{I}}_o \{ \underline{\psi}^{(n+1)} - \underline{\psi}^{(n)} \}$$

$$= \Delta \underline{\underline{I}}_o \underline{\underline{B}} \{ \underline{\underline{I}}_o \underline{\psi}^{(n+1)} + \underline{\underline{I}}_x \left[\underline{\underline{I}}+\Delta\underline{\underline{B}}\right] \underline{\psi}^{(n)} \} \tag{2.18}$$

This last step makes it simple to compute $\underline{\underline{I}}_o \underline{\psi}^{(n+1)}$ directly, since the only non-zero elements of the 5-stripe part of $\underline{\underline{I}}_o \underline{\underline{B}} \underline{\underline{I}}_o$ lie on the diagonal. This is because every o-point has 4 X-points as its immediate neighbors, and in computing the effect on leakage due to the fluxes at these neighboring points at t_{n+1}, we are using for $\underline{\underline{I}}_x \underline{\psi}^{(n+1)}$ the values estimated by (2.16). Thus the only part of $\underline{\psi}^{(n+1)}$ being treated implicitly is the central point of the five point difference scheme.

Finding the elements of $\underline{\underline{I}}_o \underline{\psi}^{(n+1)}$ is then not difficult.

Thus from Steps 1 and 2 we have $\underline{\psi}^{(n+1)}$, the sum of $\underline{\underline{I}}_x \underline{\psi}^{(n+1)}$ from Eq. (2.16) and $\underline{\underline{I}}_o \underline{\psi}^{(n+1)}$ from Eq. (2.18).

Stage 2, Steps 1 and 2.

For stage 2, we repeat steps 1 and 2 but first find $\underline{\underline{I}}_o \underline{\psi}^{(n+2)}$ from $\underline{\psi}^{(n+1)}$ and then find $\underline{\underline{I}}_x \underline{\psi}^{(n+2)}$. The relevant formulas are (2.15) and (2.18) with subscripts o and x reversed.

To show that $\underline{\psi}^{(n+2)}$ is related to $\underline{\psi}^{(n)}$ by the alternating direction form (2.14) we solve Eq. (2.18) for $\underline{\underline{I}}_0 \underline{\psi}^{(n+1)}$.

The result is

$$\underline{\underline{I}}_o \; \underline{\psi}^{(n+1)} = \left[\underline{\underline{I}}-\Delta\underline{\underline{I}}_o\underline{\underline{B}}\right]^{-1}\left[\underline{\underline{I}}_o+\Delta\underline{\underline{I}}_o\underline{\underline{B}}\underline{\underline{I}}_x+\Delta^2\underline{\underline{I}}_o\underline{\underline{B}}\underline{\underline{I}}_x\underline{\underline{B}}\right]\underline{\psi}^{(n)} \qquad (2.19)$$

Combining with (2.16) yields

$$\underline{\underline{I}}_o \; \underline{\psi}^{(n+1)} + \underline{\underline{I}}_x \; \underline{\psi}^{(n+1)} = \underline{\psi}^{(n+1)} =$$

$$= \left[\underline{\underline{I}}-\Delta\underline{\underline{I}}_o\underline{\underline{B}}\right]^{-1}\left[\underline{\underline{I}}_o+\Delta\underline{\underline{I}}_o\underline{\underline{B}}\underline{\underline{I}}_x+\Delta^2\underline{\underline{I}}_o\underline{\underline{B}}\underline{\underline{I}}_x\underline{\underline{B}} +\right.$$

$$\left. + \left(\underline{\underline{I}}-\Delta\underline{\underline{I}}_o\underline{\underline{B}}\right)\left(\underline{\underline{I}}_x+\Delta\underline{\underline{I}}_x\underline{\underline{B}}\right)\right] \underline{\psi}^{(n)}$$

or

$$\underline{\psi}^{(n+1)} = \left[\underline{\underline{I}}-\Delta\underline{\underline{I}}_o\underline{\underline{B}}\right]^{-1}\left[\underline{\underline{I}}+\Delta\underline{\underline{I}}_x\underline{\underline{B}}\right]\underline{\psi}^{(n)} \qquad (2.20)$$

Since the order of operations is inverted in Stage 2, we obtain

$$\underline{\psi}^{(n+2)} = \left[\underline{\underline{I}}-\Delta\underline{\underline{I}}_x\underline{\underline{B}}\right]^{-1}\left[\underline{\underline{I}}+\Delta\underline{\underline{I}}_o\underline{\underline{B}}\right]\underline{\psi}^{(n+1)}$$

$$= \left[\underline{\underline{I}}-\Delta\underline{\underline{I}}_x\underline{\underline{B}}\right]^{-1}\left[\underline{\underline{I}}+\Delta\underline{\underline{I}}_o\underline{\underline{B}}\right]\left[\underline{\underline{I}}-\Delta\underline{\underline{I}}_o\underline{\underline{B}}\right]^{-1}\left[\underline{\underline{I}}+\Delta\underline{\underline{I}}_x\underline{\underline{B}}\right]\underline{\psi}^{(n)} \qquad (2.21)$$

This result has the form of (2.14) if we make the splittering

$$\underline{\underline{B}}_1 = \underline{\underline{I}}_x\underline{\underline{B}}$$

$$\underline{\underline{B}}_2 = \underline{\underline{I}}_o\underline{\underline{B}} \qquad (2.22)$$

iii) The Frequency Transformation

Since alternating direction methods do not require that iterative procedures be used to invert matrices, they are inherently faster per time step than implicit schemes. Unfortunately, however, they are less accurate so that much smaller time steps must be taken to obtain an acceptably accurate prediction of how the $\phi_g(\underline{r},t)$ behave during a transient. A procedure that helps to overcome this difficulty and again make alternating direction methods competitive with implicit schemes is to apply a "frequency transformation". The essence of the idea is to replace the variables $\phi_g(\underline{r},t)$ and $C_i(\underline{r},t)$ in the time-dependent, group-diffusion equations (2.1) and (2.2) by related variables, $\psi_g(\underline{r},t)$ and $\xi_i(\underline{r},t)$, that vary more slowly in time than do the $\phi_g(\underline{r},t)$ and the $C_i(\underline{r},t)$. Then, because the ψ_g and the ξ_i do vary slowly, larger time steps may be taken in solving for them.

The transformation to more slowly varying functions is accomplished by introducing a set of position-dependent "frequencies", $\Omega_g^p(\underline{r})$ and $\Omega_i^d(\underline{r})$ (g=1,2...G; i=1,2...I) (determined as described below) such that

$$\phi_g(\underline{r},t) \equiv e^{\Omega_g^p(\underline{r})t}\psi_g(\underline{r},t)$$

$$C_i(\underline{r},t) \equiv e^{\Omega_i^d(\underline{r})t}\xi_i(\underline{r},t) \qquad (2.23)$$

Introducing this transformation into (2.1) and (2.2) yields

$$\frac{\partial}{\partial t}\left(\frac{\psi_g(\underline{r},t)}{v_g}\right) = e^{-\Omega_g^p(\underline{r},t)}\Big\{\Big[\nabla\cdot D_g(\underline{r},t)\nabla\psi_g(\underline{r},t)$$

$$- \Sigma_t(\underline{r},t)\psi_g(\underline{r},t) - \frac{\Omega_g^p(r,t)}{v_g}\psi_g(\underline{r},t)\Big] e^{\Omega_g^p(\underline{r},t)t}$$

$$+ \sum_{g'=1}^{G}\Big[\Sigma_{gg'}(\underline{r},t)+\sum_j(1-\beta^j)\chi_{pg}^j\nu\Sigma_{fg'}^j(\underline{r},t)\Big]\psi_{g'}(\underline{r},t)e^{\Omega_g^p(\underline{r},t)t}\Big\}$$

$$+ \sum_{i=1}^{I}\lambda_i e^{-\Omega_g^p(\underline{r},t)t}\chi_{ig}e^{\Omega_i^d t}\xi_i$$

$$\frac{\partial}{\partial t}\xi_i(\underline{r},t) = e^{-\Omega_i^d t}\sum_j\beta_i^j\sum_{g'=1}^{G}\nu\Sigma_{fg'}^j(\underline{r},t)\psi_{g'}(\underline{r},t)e^{\Omega_g^p(\underline{r},t)t}$$

$$- (\lambda_i + \Omega_i^d)\xi_i \quad ; \quad i = 1, 2 \ldots I \qquad (2.24)$$

Equations (2.24) have the same form as Eq. (2.1) and (2.2). However, if the frequencies $\Omega_g^p(\underline{r})$ and $\Omega_i^d(\underline{r})$ are properly chosen, $\underline{\psi}(\underline{r},t)$ and the $\xi_i(\underline{r},t)$ will vary in time much more slowly than $\underline{\phi}(\underline{r},t)$ and the $C_i(\underline{r},t)$. Thus much larger time steps can be used when solving (2.24) in finite difference form.

The selection of the proper frequencies is still somewhat of an art. Except for the trivial case of the reactor on an asymptotic period the $\phi_g(\underline{r},t)$ will not exhibit a simple exponential rise, even if the single exponent is allowed to be group and position dependent. Thus, in the general case, there is no set of frequencies such that, even during a small time step, the ψ_g and ξ_i in Eq. (2.23) will be completely independent of time. All that we can hope for is that the transformation (2.3.23) removes most of the time dependence from the ϕ_g and C_i. Thus, since the frequencies are somewhat empirical, "best-fit" numbers, current practice is to assume that the time behavior during time step n will be fairly similar to that of time step (n-1) and to determine the Ω's for the interval $t_n \rightarrow t_{n+1}$ from the known values, $\phi_g(\underline{r},t_{n-1})$, $\phi_g(\underline{r},t_n)$, $C_i(\underline{r},t_{n-1})$ and $C_i(\underline{r},t_n)$ according to the relations

$$\Omega_g^p(\underline{r},\Delta t_n) = \frac{1}{\Delta t_n} \ln \frac{\phi_g(\underline{r},t_n)}{\phi_g(\underline{r},t_{n-1})} \quad ; \quad g = 1,2...G$$

$$\Omega_i^d(\underline{r},\Delta t_n) = \frac{1}{\Delta t_n} \ln \frac{C_i(\underline{r},t_n)}{C_i(\underline{r},t_{n-1})} \quad ; \quad i = 1,2...I \qquad (2.25)$$

When Eq. (2.24) are differenced spatially, the $\underline{r}$-dependence of the frequencies reduces to there being a different set of frequencies for each mesh point. In practice it is found that, at a given mesh point, it is sufficient to use a single frequency for all energy groups ($\Omega_g^p(\underline{r},\Delta t_n) = \Omega^p(\underline{r},\Delta t_n)$; g=1,2...G). Even with this simplification computing the frequencies is a bit expensive. Moreover, for some transients (for example starting or ceasing to move a control rod) the past history provides a poor prediction of the future. When this happens, the frequencies, as predicted by Eq. (2.25) , are not optimum, and shorter time steps or iterative procedures have to be employed.

c) Alternative Methods for Solving Time Dependent Group Diffusion Equations

The finite difference approach to solving the time dependent group diffusion equations is quite practical for one dimensional geometries and can provide numerical standards against which to validate more approximate two and three dimensional solution methods by applying them to small test problems. However, if more than about 20000 spatial mesh points are required for reasons of accuracy or in order to represent geometrical detail, the finite difference approach becomes extremely expensive. Thus more efficient methods must be used for an accurate analysis of large LWR's.

Fortunately all the advanced methods discussed in connection with the static equations can be extended to the time-dependent case. For the response matrix technique it is necessary to define time dependent response matrices [25] and this becomes complicated when feedback effects must be accounted for [26]. The extension of the synthesis scheme is more straightforward: the mixing functions $T_h^g(z)$ of (1.57) simply become time-dependent

$$\phi_g(x,y,z,t) = \sum_{k=1}^{K} \psi_k^g(x,y)\, T_k^g(z,t) \qquad (2.26)$$

The resulting equations can be solved as if they were one-dimensional, time dependent finite difference equations. One serious potential problem arises with the time dependent synthesis method. The expansion functions $\psi_k^g(x,y)$ must be able to represent any tilting effects occurring during the course of the transient. Use of multichannel synthesis methods may be very helpful for such situations since if flux tilting in the radial plane occurs, they will provide it automatically even if such tilting has not been anticipated.

Extension of the finite element and nodal methods to time dependent situations is also straightforward [27, 16, 17, 18]. Of the two, the nodal schemes seem to be much faster. In fact the nodal method appears today to be the most efficient procedure for solving the time-dependent group diffusion equations.

2.2 The Point Kinetics Method

For many reactor transients the shape of the neutron flux (as opposed to its magnitude) changes only slightly. For such transients the "point kinetics equations" provide an accurate and extremely simple method by which to predict the detailed space and time behavior of the neutron population. To those familiar with elementary derivations of the point kinetics equations this statement may be surprising. Nevertheless, the statement is true. For many situations the point kinetics equations can provide an excellent solution of the time-dependent group diffusion equations (2.1, 2.2) . They are in no way limited to a "point" or to a one-speed or one-group reactor model. In fact a formal manner, the point equations can be obtained from the time dependent Boltzmann transport equation without making any approximations at all.

a) Derivation of the Point Kinetics Equations

Because the algebraic manipulations are a bit simpler to follow we shall derive the point kinetics equations starting from the continuous space-time-energy diffusion equations. These may be written

$$\frac{\partial}{\partial t}\left[\frac{1}{v(E)}\,\phi(\underline{r},E,t)\right] = \sum_g \chi_p^j(E)(1-\beta^j)\int_o^\infty \nu\Sigma_f(\underline{r},E',t)\,\phi(\underline{r},E',t)dE'$$

$$+ \sum_i \chi_i(E)\lambda_i c_i(\underline{r},t) + \nabla\cdot D(\underline{r},E)\nabla\phi(\underline{r},E,t) - \Sigma_t(r,E,t)\phi(\underline{r},E,t)$$

$$+ \int_o^\infty \Sigma_p(\underline{r},E'\to E,t)\,\phi(\underline{r},E',t)dE'$$

$$\frac{\partial c_i(\underline{r},t)}{\partial t} = \sum_j \beta_i^j \int_o^\infty \nu\Sigma_f{}^j(\underline{r},E',t)\phi(\underline{r},E',t)dE' - \lambda_i c_i(\underline{r},t)$$

$$i = 1, 2\ldots I \qquad (2.27)$$

To reduce the algebraic complexity we introduce the net absorption operator A and the fission neutron production operator F^j defined by their operation on any function $f(\underline{r},E,t)$ by

$$Af \equiv \Sigma_t(\underline{r},E,t)f(\underline{r},E,t) - \int_o^\infty \Sigma_s(\underline{r},E'\to E,t)f(\underline{r},E',t)dE'$$

$$F^j f \equiv \int_o^\infty \nu\Sigma_f{}^j(\underline{r},E',t)\,f(\underline{r},E',t)\,dE' \qquad (2.28)$$

In terms of these operators and with all functional dependence repressed (2.27) take on the form

$$\frac{1}{v}\frac{\partial\phi}{\partial t} = \nabla\cdot D\nabla\phi - A\phi + \sum_j \chi_p^{\,j}(1-\beta^j)F^j\phi + \sum_i \chi_i\lambda_i c_i$$

$$\frac{\partial c_i}{\partial t} = \sum_j \beta_i^{\,j}F^j\phi - \lambda_i c_i \; ; \quad i = 1, 2, \ldots I \tag{2.29}$$

The quantity of first importance in neutron kinetics is the instantaneous total neutron population in the reactor. We define as the unknown function to be obtained from solving the point kinetics equations a closely related quantity T(t):

$$T(t) \equiv \int_{\text{reactor}} dV \int_0^\infty dE\; W(\underline{r},E)\,\frac{1}{v(E)}\,\phi(\underline{r},E,t) \tag{2.30}$$

where $W(\underline{r},E)$ is a time-independent weight function introduced for reasons which will become clear shortly. (Note that if $W(\underline{r},E) = 1$, T(t) is the total neutron population in the reactor at time t.)

Having defined an "amplitude function" T(t) we next define a (time dependent) "shape function" $S(\underline{r},E,t)$ by the relationship

$$S(\underline{r},E,t)\; T(t) \equiv \phi(\underline{r},E,t) \tag{2.31}$$

Substitution of the expression into (2.30) and division by T(t) yields

$$1 = \int_{\text{reactor}} dV \int_0^\infty dE\; W(\underline{r},E)\,\frac{1}{v(E)}\,S(\underline{r},E,t) \tag{2.32}$$

Thus the definitions (2.30) and (2.31) imply a kind of time-dependent normalization for $S(\underline{r},E,t)$ such that the integral in (2.32) is independent of time even though $S(\underline{r},E,t)$ is not.

To obtain the point kinetics equations in a formal manner we now substitute (2.31) into (2.29), multiply the results by $W(\underline{r},E)$ ($W(\underline{r},E)\chi_i(E)$ for the precurser equations) and integrate over all energy and over the entire volume of the reactor (out to where $\phi(\underline{r},E,t)$ can be set to zero). If (to get the customary form) we add and subtract $\sum_i' \chi_i\beta^j F^j\phi$ in the first of Eq. (2.29) and define the total fission spectrum for isotope j as

$$\chi^j(E) \equiv \chi_p^{(j)}(E)(1-\beta^j) + \sum_i \chi_i(E)\beta_i^{\,j} \tag{2.33}$$

we obtain

$$\int dV\int dEW\left[\nabla\cdot D\nabla S - AS + \sum_j \chi^j F^j S\right] T(t) - \int dV\int dEW\left[\sum_{i,j}\chi_i\beta_i^{\,j}F^jS\right]T(t)$$

$$+ \sum_{i=1}^{I}\lambda_i\left[\int dV\int dEW\chi_i c_i(t)\right] = \frac{\partial}{\partial t}\left[\int dV\int dEW\,\frac{1}{v}ST(t)\right] =$$

$$= \left[\int dv \int dEW \frac{1}{v} S\right] \frac{dT(E)}{dt} \quad ;$$

$$\left[\int dv \int dEW \chi_i \sum_j \beta_i{}^j F^j S\right] T(t) - \lambda_i \left[\int dv \int dEW \chi_i c_i(t)\right] =$$

$$= \frac{\partial}{\partial t} \left[\int dv \int dEW \chi_i c_i(t)\right] =$$

$$= \left[\int dv \int dEW \frac{1}{v} S\right] \frac{d}{dt} \left[\frac{\int dv \int dEW \chi_i c_i(t)}{\int dv \int dEW \frac{1}{v} S}\right] \qquad (2.34)$$

where the second equalities are valid since (2.32) shows that $\int dv \int dEW \frac{1}{v} S(\underline{r},E,t)$ is not a function of time.

If now we divide by $\int dv \int dEW \sum_j \chi^j F^j S$ and define

$$\rho(t) \equiv \frac{\int dv \int dEW \left[\nabla \cdot D\nabla S - AS + \sum_j \chi^j F^j S\right]}{\int dv \int dEW \sum_j \chi^j F^j S} \qquad (2.35)$$

$$\beta_i(t) \equiv \frac{\int dv \int dEW \sum_i \chi_i \beta_i{}^j F^j S}{\int dv \int dEW \sum_j \chi^j F^j S} \quad ; \quad \beta(t) \equiv \sum_{i=1}^{I} \beta_i{}^j(t) \qquad (2.36)$$

$$\Lambda(t) \equiv \frac{\int dv \int dEW \frac{1}{v} S}{\int dv \int dEW \sum_j \chi^j F^j S} \qquad (2.37)$$

Along with

$$C_i(t) \equiv \frac{\int dv \int dEW(\underline{r},E) \chi_i(E) c_i(\underline{r},t)}{\int dv \int dEW \frac{1}{v} S} \qquad (2.38)$$

we obtain, after some rearrangement, the point kinetics equations:

$$\frac{dT(t)}{dt} = \frac{\rho-\beta}{\Lambda} T(t) + \sum_i \lambda_i C_i(t)$$

$$\frac{dC_i(t)}{dt} = \frac{\beta_i}{\Lambda} T(t) - \lambda_i C_i(t); \quad i = 1, 2, \ldots 5 \qquad (2.39)$$

Since we have derived them only by making definitions rather than approximations, the point kinetics equations are formally as accurate as the space-dependent equations from which they were derived. However, the "kinetics parameters" $\rho(t)$ (reactivity), $\beta_i(t)$ (effective delayed neutron fraction of the i^{th} precursor group) and $\Lambda(t)$ (prompt neutron lifetime) depend on the shape function $S(\underline{r},E,t)$ and hence on $\phi(\underline{r},E,t)$.

Thus the practical utility of (2.39) depends on how well $S(\underline{r},E,t)$ can be approximated by some simple procedure.

The solution of (2.39) by finite difference methods is straightforward and inexpensive. Since they have the form of (2.8) with all the $\underline{B}_{ij}$'s reduced to numbers, the "θ-method" (Eq. 2.1, 2.22) extended to I delayed groups, is readily applicable. Taking $\theta_p = 1$ and the θ_d's (there are now I of them) = 1/2 usually provides the best combination of accuracy and economy. However, if great accuracy is desired or if the reactor is super prompt critical so that the correct representation of a fast rising exponential $\sim e^{(\frac{\rho-\beta}{\Lambda})t}$ is important $\theta_p = \theta_d = 1/2$ is preferred. A Taylor series expansion shows that forthat choice the equations converge fastest as the time step size shrinks to zero.

Analytical solutions of (2.39) are simple only if ρ, β and Λ are constant, and ρ is rarely constant during power reactor transients. Thus such solutions are primarily useful in illustrating the qualitative behavior of reactor transient (something with which it is assumed the reader is already familiar).

b) <u>The Choice of the Weight Function $W(\underline{r},E)$; The Adjoint Flux</u>

The kinetics parameters ρ, Λ and the β_i (Eq. 2.35-7) depend on the time-dependent shape function $S(\underline{r},E,t)$, and some approximation to this shape must be made if practical use is to be made of the point kinetics equations. The simplest choice is to approximate $S(\underline{r},E,t)$ by $S_o(\underline{r},E)$ the static flux shape associated with some reference state of the reactor under consideration. The shape $S_o(\underline{r},E)$ is thus a solution of the time independent counterpart of (2.29).

$$\nabla\cdot D_o'\nabla S_o - A_o S_o + \frac{1}{\lambda_o}\sum_j \chi^j F_o^j S_o = 0 \qquad (2.40)$$

where subscript zero indicates that the relevant cross sections refer to some time-independent reference state and the eigenvalue λ_o is included since this state may not correspond to a critical condition for the actual reactor. (The flux shape associated with a perturbed reactor condition may better represent $S(\underline{r},E,t)$ throughout most of the transient being analysed.)

If we then select $S_o(\underline{r},E)$, the error $\delta S(\underline{r},E,t)$ resulting from this selection will be defined by

$$S(\underline{r},E,t) \equiv S_o(\underline{r},E) + \delta S(\underline{r},E,t) \qquad (2.41)$$

Examination of the definitions of Λ(t) and the $\beta_i(t)$ (eqs. 2.36,.37) shows that, if δS is small (and $W(\underline{r},E) > 0$) the errors in Λ and the β_i will also be small. Thus the practice of assuming that Λ and the β_i are constant parameters determined for the reference state is usually quite valid.

For reactivity, the situation is different. Reactivity is zero for a critical condition so that, if, for example, it

is changed by a perturbation in the cross sections specifying the operator $A(A_o \rightarrow A_o + \delta A)$ and if that same perturbation changes the shape function $S(S_o \rightarrow S_o + \delta S)$, the resultant contribution to the change in reactivity will come from the terms $-W(\delta A)S_o - WA_o\delta S$ in (2.35) . If it is necessary to neglect $WA_o\delta S$ (δS being unknown) the resultant error could be of the same magnitude as $W(\delta A)S_o$, the term being used to compute $\rho(t)$.

It is to overcome this problem that we have introduced the weight function $W(\underline{r},E)$. It is possible to select it so that all the first order error terms in (2.35) involving δS vanish. The procedure is a standard one in mathematical physics and consists of selecting $W(\underline{r},E)$ to be the solution $\phi_o^*(\underline{r},E)$ of the equation that is mathematically "adjoint" to the equation (2.40) specifying the static reference state.

The equation adjoint to (2.40) can be obtained by reversing the E and E' in the operators A and $\sum_j \chi^j F^j$ (Eq. 2.28) . Thus, we first define an operator

$$M \equiv \sum_j \chi^j F^j \tag{2.42}$$

so that (2.40) becomes

$$\nabla\cdot D_o\nabla S_o - A_oS_o + \frac{1}{\lambda_o} M_o S_o = 0 \tag{2.43}$$

We next define adjoint operators A_o^* and M_o^* by their operation on any function $f^*(\underline{r},E)$

$$A_o^*f^* \equiv \Sigma_{t_o}(r,E)f^*(\underline{r},E) - \int_o^\infty \Sigma_{s_o}(\underline{r},E \rightarrow E')f^*(\underline{r},E')dE'$$

$$M_o^*f^* \equiv \int_o^\infty \sum_j \chi^j(E')\nu\Sigma^j(\underline{r},E)f^*(\underline{r},E')dE' \tag{2.44}$$

The equation mathematically adjoint to (2.43) is

$$\nabla\cdot D_o\nabla\phi_o^* - A_o^*\phi_o^* + \frac{1}{\lambda_o} M_o^* \phi_o^* = 0 \tag{2.45}$$

The solution conditions imposed on $\phi_o^*(\underline{r},E)$ are the same as those imposed on $\phi_o(\underline{r},E)$, namely, ϕ_o^* and the normal component of $D_o\nabla\phi_o^*$ across internal interfaces are to be continuous, and ϕ_o^* is to be non-negative in the interior of the reactor and is to vanish on the outer surface. For these conditions the eigenvalues λ_o in (2.45) and (2.43) can be shown to be the same.

To apply the adjoint equation to remove terms of order δS in the expression for ρ we multiply (2.45) by $S(\underline{r},E,t)$ and integrate over energy and reactor volume. Since the result of the manipulation is still zero, we can subtract it from (2.35) (with $W(\underline{r},E)$ taken as $\phi_o^*(\underline{r},E)$) to obtain

$$\rho(t) = \frac{\int dV \int dE \;\; \phi_o^*(\nabla\cdot D\nabla S - AS + MS) \;-\; S(\nabla\cdot D_o\nabla\phi_o^* - A_o^*\phi_o^* + \frac{1}{\lambda_o} M_o^*\phi_o^*)}{\int dV \int dE \; \phi_o^* \; M \; S} \tag{2.46}$$

Now by the chain law of differentiation we have

$$\int \nabla\cdot(\phi_o^* D\nabla S)dV = \int (\nabla\phi_o^*)\cdot(\nabla S)dV + \int \phi_o^* \nabla\cdot(D\nabla S)dV \tag{2.47}$$

But, since $(\phi_o^* D\nabla S)$ is continuous across all internal interfaces, application of Gauss's Law to the divergence term yields

$$\int \nabla\cdot \phi_o^* D\nabla S \; dV = \S(\phi_o^* D\nabla S)\cdot \underline{N} dS \tag{2.48}$$

where the surface integral in over the outer surface of the reactor only. Since ϕ_o^* vanishes on the outer surface this integral alsc vanishes and (2.47) yields

$$\int \phi_o^* \nabla\cdot(D\nabla S)dV = -\int D\nabla\phi_o^*\cdot\nabla S dV \tag{2.49}$$

Similarly, since $SD\cdot\nabla\phi_o^*$ is continuous across interval interfaces

$$\int S\nabla\cdot(D_o\nabla\phi_o^*)dV = -\int D_o\nabla S\cdot\nabla\phi_o^* \; dV \tag{2.50}$$

Finally, since

$$\int_o^\infty dE \int_o^\infty dE' \; S(\underline{r},E,t) \; \Sigma_{s_o}(\underline{r},E\to E')\phi_o^*(\underline{r},E') =$$

$$= \int_o^\infty dE \int_o^\infty dE' \; \phi_o^*(\underline{r},E) \; \Sigma_{s_o}(\underline{r},E'\to E) \; S(\underline{r},E',t) \tag{2.51}$$

and

$$\int_o^\infty dE \int_o^\infty dE' \; S(\underline{r},E,t) \; \Sigma' \chi^j(E')\nu\Sigma_f{}^j(\underline{r},E)\phi_o^*(\underline{r},E') =$$

$$= \int_o^\infty dE \int_o^\infty dE' \phi_o^*(\underline{r},E) \; \Sigma_j \chi^j(E)\nu\Sigma_f{}^j(\underline{r},E') \; S(\underline{r},E',t) \tag{2.52}$$

we have

$$\int dV \int dE \; SA_o^* \; \phi_o^* = \int dV \int dE \; \phi_o^* \; A_o S$$

$$\int dV \int dE \; S \; M_o^* \; \phi_o^* = \int dV \int dE \; \phi_o^* \; M_o \; S \tag{2.53}$$

Thus, without approximation (2.3.46) becomes

$$\rho(t) = \frac{\int dV \int dE \left[-\delta D\nabla\phi_o^*\cdot\nabla S - \phi_o^* \; \delta A \; S + \phi_o^* \; \delta M \; S\right]}{\int dV \int dE \; \phi_o^* \; M \; S} \tag{2.54}$$

where

$$\delta D \equiv D(\underline{r},E,t) - D_o(\underline{r},E)$$

$$\delta A \equiv \Sigma_t(\underline{r},E,t) - \Sigma_{t_o}(\underline{r},E) + \int dE' \left[\Sigma_s(\underline{r},E'\to E,t) - \Sigma_{s_o}(\underline{r},E')\right] \ldots$$

$$\delta M \equiv \int dE' \sum_j \chi^j \left[\nu\Sigma_f{}^j(\underline{r},E',t) - \frac{1}{\lambda_o}\nu\Sigma_{t_o}{}^j(\underline{r},E')\right] \quad \ldots \qquad (2.55)$$

If now we approximate S by S_o, a perturbation δA contributes a principle part $\phi_o^*\delta AS$ to ρ and requires neglecting only a second order term $\phi_o^*\delta A\delta S$. Thus use of the adjoint flux as weight function increases the accuracy of computations of $\rho(t)$ made using an approximation to $S(\underline{r},E,t)$.

c) Neutron Importance - Physical Significance of the Kinetics Parameters

The adjoint function $\phi_o^*(\underline{r},E)$ has a physical interpretation[28] which in turn leads to a precise physical interpretation of the point kinetics parameters. This interpretation is given in terms of a hypothetical experiment as follows:

Introduce a sample of η neutrons (η being large enough so that statistical fluctuations may be ignored but small enough so that no feedback effects occur) into the reference critical reactor at some point $\underline{r}$. Let the neutrons in the sample all have energy E and be travelling in directions that are isotropically distributed. Since the reactor is critical, the ultimate consequence (after equilibrium has again been restored) of introducing the η neutrons will be an increase in the total steady state neutron population of the critical reactor from N_o to $N_o + \Delta N$. The magnitude of ΔN will depend on where and with what energy the neutrons were introduced ($\Delta N = \Delta N(\underline{r},E)$). It turns out to be possible to show [3] that with proper normalization

$$\phi_o^*(\underline{r},E) = \frac{1}{\eta}\Delta N(\underline{r},E) \qquad (2.56)$$

In words, the adjoint flux $\phi_o^*(\underline{r},E)$ in a critical reactor is the asymptotic increase in the total neutron population of the reactor due to the introduction at $\underline{r}$ of an average neutron out of a sample all having energy E and an isotropic distribution of directions of travel. Because of this interpretation $\phi_o^*(\underline{r},E)$ is called the *importance* in the critical reference reactor of a neutron at $\underline{r}$ having energy E.

With this interpretation of importance and with $W(\underline{r},E)$ in all definitions replaced by $\phi_o^*(\underline{r},E)$ the physical significance of the point kinetics parameters can be interpreted as follows:

T(t) (Eq. 2.39) is the total importance in the reference reactor of all the neutrons present at time t in the perturbed reactor.

$C_i(t)$ (Eq. 2.37) along with 2.32 is the importance in the reference reactor of all the neutrons that would appear if the $C_i(\underline{r},t)$ decayed instantly at time t.

$\rho(t)$ (Eq. 2.35) is the net rate of the production of importance in the reference reactor assuming delayed neutrons appear instantly divided by the rate at which importance is produced in the reference reactor by the fission process at time (t) - again assuming delayed neutrons appear instantly (χ^j - Eq. 2.33 is the total spectrum). This interpretation comes from multiplying numerator and denominator of (2.35) by T(t) and then replacing ST by $\phi(\underline{r},E,t)$; $\nabla\cdot D\phi - A\phi + \Sigma_j \chi^j F^j \phi$ dVdE is then the net "instantaneous" production rate of neutrons into dVdE and multiplication by $W(\underline{r},E) = \phi_o^*(\underline{r},E)$ followed by integration over all $\underline{r}$ and E yields the rate at which these neutrons would produce importance in the reference reactor.

$\beta_i(t)$ is the "instantaneous" rate at which the i^{th} precursor group would produce importance in the reference reactor divided by the corresponding instantaneous importance production rate for all neutrons appearing from fission at time t.

$\Lambda(t)$ (Eq. 2.37) is a characteristic lifetime of the importance of all the neutrons present in the reactor at time t. This interpretation is not as precise as the others except for the reference reactor. For this critical case the creation rate of importance must equal its decay rate and we have from (2.37).

$$\int dV \int dE \phi_o^* M_o \phi_o = \frac{1}{\Lambda} \int dV \int dE\ \phi_o^* \frac{1}{v} \phi_o \qquad (2.57)$$

Thus the decay rate of importance equals the total importance present divided by a time constant.

The more elementary notions of the kinetics parameters can now be seen in relation to the precise interpretation just given. Thus T(t) is usually thought of as total reactor power. This is only an approximate interpretation unless $W(\underline{r},E)$ is taken as $\nu(E)\Sigma_f(\underline{r},E)$ (2.39) . The reactivity is often thought of as the fractional change in the net numbers of neutrons produced per generation. If $W(\underline{r},E) = 1$, this is an approximately valid interpretation (although it is difficult to define a "generation" for a reactor in a changing transient state). Similarly the usual notion that the prompt neutron lifetime is the average time that fission neutrons live once they appear is more justified if $W(\underline{r},E) = 1$.

d) Computation and Measurement of Reactivity

The simplest choice for the shape function $S(\underline{r},E,t)$ is $S_o(\underline{r},E)$, the static flux shape in the reference reactor. When this choice is made Eq. (2.54) becomes the "perturbation formula for reactivity". This perturbation formula has the extremely important property that the reactivity changes due to different perturbations are additive. Thus if ρ_1 is the reactivity change due to perturbing only A an amount δA_1; ρ_2 is that due to perturbing only M by δM_2, and ρ_3 is that due to the perturbation $(\delta A_1 + \delta M_2)$. ρ_3 will equal $\rho_1 + \rho_2$ provided - and only provided - the same shape function $S_o(\underline{r},E)$

is used for all three perturbations. It is important to remember that this additivity is lost if a time-dependent shape function is used.

A more accurate choice of shape function is provided by the "adiabatic approximation". Here the shape is the solution of

$$\nabla\cdot D(t)\nabla S_\lambda - A(t)S_\lambda + \frac{1}{\lambda_t} M(t)\, S_\lambda = 0 \qquad (2.58)$$

where the diffusion coefficient D(t) and the operators A(t) and M(t) are those appropriate to the reactor condition at time t and λ_t is adjusted to make the reactor artificially critical at that time.

Substituting (2.58) into (2.35) gives

$$\rho_\lambda(t) = \frac{\int dV \int dE\; W \left[-\frac{1}{\lambda_t} M + M \right] S_\lambda}{\int dV \int dE\; W\, M\, S_\lambda} = 1 - \frac{1}{\lambda_t} \qquad (2.59)$$

This expansion for reactivity is often called the "static reactivity" since it is most often used to compare the results of a sequence of static calculations.

For dynamic problems ρ_λ is not very useful since it requires that static solutions of (2.58) be obtained frequently and since S_λ does not account for the fact that the shape of the delayed precursor population changes more slowly in time than does the flux itself. A more accurate procedure is to compute $\rho(t)$ by the "quasi-static method" [29]. In this method values of $S(\underline{r},E,t)$ are recomputed periodically in such a way that both the instantaneous reactor conditions and the instantaneous precursor concentration distributions are accounted for. The essential assumption is that at a time, t_n, when this recomputation is made

$$\frac{1}{c_i(\underline{r},t_n)} \frac{\partial c_i(\underline{r},t_n)}{dt} = \frac{1}{C_i(t_n)} \frac{d\, C_i(t_n)}{dt} \equiv \omega_i$$

$$\frac{1}{\phi(\underline{r},E,t_n)} \frac{\partial \phi(\underline{r},E,t_n)}{\partial t} = \frac{1}{T(t_n)} \frac{dT(t_n)}{dt} \equiv \omega_p$$

$$\text{all } \underline{r} \qquad (2.60)$$

The ω_i and ω_p are found from the point equation solution just prior to time t. Then, if t_{n-1}, was the last time a space dependent solution was obtained we assume that

$$c_i(\underline{r},t_n) = \frac{C_i(t_n)}{C_i(t_{n-1})}\, c_i(\underline{r},t_{n-1}) \qquad (2.61)$$

Substitution of (2.60) and (2.61) into the first of Eq. (2.29) then yields the inhomogeneous equation for ϕ at t_n.

$$\frac{\omega_p}{v}\phi - \nabla\cdot D\nabla\phi + A\phi - \sum_j \chi_p^i(1-\beta^j)F^j\phi =$$

$$= \sum_i \chi_i\lambda_i \frac{C_i(t_n)}{C_i(t_{n-1})} \; c_i(\underline{r},t_{n-1}) \qquad (2.62)$$

The second of Eq. (2.29) together with (2.62) then permit an updating of the $c_i(\underline{r},t)$

$$c_i(\underline{r},t_n) = \frac{1}{\omega_i+\lambda_i} \sum_j \beta_i{}^j \, F^j(t_n) \; \phi(t_n) \qquad (2.63)$$

The quasi static method is really an approximate way of solving (2.40) . If time steps are small and the shape functions are updated every time step it converges to an exact solution. Its great advantage for practical problems is that for many cases the updating can be very infrequent.

The simplest way to infer reactivity experimentally is by an "asymptotic period" measuremnet. As the name implies, one introduces a step perturbation the reactivity worth of which is to be measured and waits until the flux level is rising everywhere as $e^{\omega t}$. Then $\frac{dT}{dt} = \omega T$; $\frac{d\,C_i}{dt} = \omega C_i$ and (2.39) can be manipulated to give

$$\rho = \omega\Lambda + \sum_i \frac{\omega\,\beta_i}{\omega+\lambda_i} \qquad (2.64)$$

Provided Λ and the β_i are known from a calculation, measurement of ω then leads to a value of ρ. Equation (2.64) is the "inhour formula" for reactivity.

The inhour formula cannot be used to infer large negative values of reactivity since then ω is so close to the negative of the smallest λ_i that experimental error becomes very large. For this situation a technique known as the "rod-drop" method is sometimes useful.

In the rod-drop method one is interested in inferring the decreasing reactivity when one or more control rods is inserted into the reactor. If it is assumed that the counting rate D(t) of a neutron detector is proportional to T(t) (D(t) = αT(t)), the initial count rate for the critical reactor

($\rho = \frac{dT(0)}{dt} = \frac{dC_i(0)}{dt} = 0$) is from (2.39)

$$\frac{\beta}{\Lambda}\ \frac{1}{\alpha}\ D(0) = \sum_i \lambda_i\ C_i(0) \qquad (2.65)$$

If the rods are then dropped into the core, there is a very brief time during which the prompt neutrons readjust and T(t) falls abruptly. However it quickly levels off to a new value T(0+) and $\frac{dT(t)}{dt}$ then becomes small in comparison with either term on the right hand side of the first of (2.39) . Moreover, since the delayed precursors decay very little in the brief time, $C_i(0+)$ is very little different from $C_i(0)$. Thus we have from (2.39) and (2.65).

$$0 \simeq \frac{\rho(0+)-\beta}{\Lambda}\ \frac{1}{\alpha}\ D(0+) + \sum_i \lambda_i\ C_i(0+)$$

$$\simeq \frac{\rho(0+)-\beta}{\Lambda}\ \frac{1}{\alpha}\ D(0+) + \frac{\beta}{\Lambda}\ \frac{1}{\alpha}\ D(0) \qquad (2.66)$$

Hence

$$\frac{\rho(0+)}{\beta} = -\frac{D(0) - D(0+)}{D(0+)} \qquad (2.67)$$

and if β is known ρ(0+) can be inferred from the counting rates before and just after the rod-drop.

Experiments of this kind involving potentially large changes in flux shape must be analysed with great caution. Equation (2.67) is likely to be in serious error since we have tacidly assumed in deriving it that β, Λ and α after the drop are the same as before. However, that will only be true in the unlikely event that reactor flux shapes are unchanged. Thus careful theoretical corrections must be made to analyse the rod drop experiment correctly. For the same reasons one should not expect the reactivity inferred to equal $(1 - \frac{1}{\lambda_t})$.

2.3 Feedback Effects

So far no explicit indication has been given of how the time dependence of the group parameters and the reactivity is to be determined. In so far as changes are externally imposed (as with variations in control rod positions or soluble poison concentration) accounting for alterations in the group parameters is straightforward. Appropriate cross sections with and without control rods present or for various concentrations of soluble poison are generated, and the values to be used when the rod is partly inserted in a node or mesh cube or when some intermediate poison concentration is present are determined by interpolation.

If the parameters vary because of local temperature or density changes, the problem becomes non-linear since changes in the local flux levels are in turn what induce the local

temperature and density variations. As with the non-linear fuel depletion situation this problem is today attached by running nuclear and thermal-hydraulic computations in tandom (although several nuclear time steps may be taken per thermal hydraulic time step). Thus it is necessary to augment the group diffusion equations or point kinetics equations with a model of thermal-hydraulic behavior in the core.

Generally the nuclear and thermal-hydraulic model interact at only two points. The nuclear model accepts nodal average temperature and densities at the beginning of a time step, assumes these quantities remain constant during the time step and supplies the thermal-hydraulic model with nodal averaged powers at the end of the time step (or of several time steps). In complementary fashion, the thermal-hydraulic model accepts the average nodal powers, assumes they stay constant during a time step and supplies the nuclear model with up-dated temperatures and densities at the end of the time step. There are some indications that a tighter coupling between the two models might lead to a more efficient overall calculation, but the matter is unresolved at present.

In any event the nuclear model receives nodal fuel temperatures, coolant temperatures and coolant densities, and the effect of these on group parameters or on reactivity must be taken into account.

For the full space dependent calculations changes in the group parameters enter the calculation directly and, as with the depletion problem, a table look-up method can be set-up to circumvent the need to do frequent neutron spectrum computations. Depending on the sensitivity to changes in thermal-hydraulic properties, the tables may be for macroscopic parameters or for microscopic fitted cross sections (Eq. 1.94). For some parameters it may be necessary to use two dimensional tables. (The microscopic nodal-averaged fission cross section for U^{235} in the resonance region may depend significantly both on the fuel temperature and the coolant density.) Alternatively, it may be possible to fit the group parameters to low order polynomials in the thermal variables. Both the table look-up and polynomial procedures thus involve complicated computer programming and the running of many auxiliary computations prior to performing any nuclear transient calculations.

With the point kinetic model it is possible to precompute directly the dependence of reactivity on the thermal parameters. To do this, we first assume that the perturbation formula for reactivity is valid so that $S(\underline{r},E,t)$ in (2. 54) may be replaced by a constant shape $S_o(\underline{r},E)$. Then we partition the total reactivity change $\rho(t)$ into contributions $\rho_n(t)$ from each of the N thermal-hydraulic nodes comprising the reactor. Thus we define

$$\rho_n(t) \equiv \frac{\int_{V_n} dV \int dE \left[- \delta D \nabla \phi_o^* \cdot \nabla S_o - \phi_o^* \delta A S_o + \phi_o^* \delta M S_o \right]}{\int_V dV \int dE \; \phi_o^* M S_o} \qquad (2.68)$$

$$n = 1, 2, \ldots N$$

where the volume integral in the numerator is over the n^{th} node while that in the denominator is over the entire reactor. (In practice the integral over energy would be a sum over energy groups. We shall retain the simpler intergral notation.) Since $S_o(\underline{r},E)$ is being used as the shape function for all perturbations, the additivity property holds, and

$$\rho(t) = \sum_{n=1}^{N} \rho_n(t) \tag{2.69}$$

The nodal reactivities, ρ_n, may be found by table look-up. However, it is more common to define local temperature and density coefficients $\frac{\partial \rho_n}{\partial \theta_n^c}\Big|_{d^c}$, $\frac{\partial \rho_n}{\partial \theta_n^f}\Big|_{P}$, $\frac{\partial \rho_n}{\partial d_n^c}\Big|_{\theta^c}$, where θ^c, d^c and θ^f are respectively coolant temperature, coolant density and fuel temperature and subscripts n indicate an average value for node n. Note that here the temperature coefficient of the coolant is at constant coolant density whereas that of the fuel is at constant pressure. Theoretical expressions for these coefficients may be obtained directly from (2.68). For example,

$$\frac{\partial \rho_n}{\partial \theta_n^c}\Big|_{d^c} = \frac{\int_{V_n} dV \int dE \left[-\frac{\partial D}{\partial \theta_m^c}\Big|_{d^c} \nabla\phi_o^* \cdot \nabla S_o - \phi_o^* \left(\frac{\partial A}{\partial \theta_n^c} - \frac{\partial M}{\partial \theta_n^c} \right)\Big|_{d^c} S_o \right]}{\int dV \int dE \; \phi_o^* \, M \, S_o} \tag{2.70}$$

where, for example, $\frac{\partial A}{\partial \theta_n^c}\Big|_{d^c}$ is the change in the operator A for node-n from its value for the reference core due to a unit change (at constant coolant density) in coolant temperature of node-n from that of the reference core. The local temperature and density coefficients themselves may depend on the thermal conditions and thus may have to be put in tables.

From the foregoing it follows that if nodal temperatures and densities differ from those of the reference core at time t by amounts $\Delta\theta_n^c(t)$, $\Delta\theta_n^f(t)$ and $\Delta d_n^c(t)$, the reactivity at time t can be determined as

$$\rho(t) = \left[\sum_{n=1}^{N} \frac{\partial \rho_n}{\partial \theta_n^c}\Big|_{d^c} \Delta\theta_n^c(t) + \frac{\partial \rho}{\partial \theta_n^f}\Big|_{P} \Delta\theta_n^f(t) + \frac{\partial \rho_n}{\partial d_n^c}\Big|_{\theta^c} \Delta d_n^c(t) \right] \tag{2.71}$$

If the $\Delta\theta$'s and Δd are the same for all nodes or if we use an average value (a questionable procedure) temperature and density coefficients for the whole core ($\sum_n \frac{\partial \rho_n}{\partial \theta_n^c}\Big|_{d^c} \equiv \frac{\partial \rho}{\partial \theta^c}\Big|_{d^c}$, etc.) can be used and (2.27) reduces to

$$\rho(t) = \frac{\partial \rho}{\partial \theta^c}\Big|_{d^c} \Delta\theta^c(t) + \frac{\partial \rho}{\partial \theta^f}\Big|_{P} \Delta\theta^f(t) + \frac{\partial \rho}{\partial d^c}\Big|_{\theta^c} \Delta d^c(t) \tag{2.72}$$

Further, if there is no boiling and θ^c, d^c and P are related by an equation of state, we can define a coolant temperature coefficient at constant pressure

$$\frac{\partial \rho}{\partial \theta^c}\Big|_{P} = \frac{\partial \rho}{\partial \theta^c}\Big|_{d^c} + \frac{\partial \rho}{\partial d^c}\Big|_{\theta^c} \frac{\partial d^c}{\partial \theta^c}\Big|_{P} \tag{2.73}$$

It is this quantity that is usually referred to as "the temperature coefficient of the coolant".

Finally, if $\Delta\theta^c = \Delta\theta^f$ we can define a "reactor temperature coefficient" $\frac{\partial\rho}{\partial\theta}\Big|_p$ such that

$$\rho(t) = \frac{\partial\rho}{\partial\theta}\Big|_p \Delta\theta(t) \qquad (2.74)$$

Thus there are many approximate ways of determining reactivity changes due to changes in thermal conditions. In practice Eq. (2.72) seems to be used most frequently. This is surprising since use of (2.71) involves very little more computing effort and the result is more accurate.

REFERENCES

1. Richard S. Varga, Matrix Iterative Analysis, Prentice-Hall Englewood Cliffs, N.J. (1962).
2. J.B. Yasinsky and S. Kaplan, "Synthesis of Three Dimensional Flux Shapes Using Discontinuous Sets of Trial Functions", Nuc. Sci. Eng. 25, 426 (1967).
3. A.F. Henry, Nuclear-Reactor Analysis (Cambridge, MA: MIT Press), 1975.
4. W.M. Stacey, Jr., "Variational Methods in Nuclear Reactor Physics", (New York, NY: Academic Press), 1974.
5. E.L. Wachspress, Variational Methods and Neutron Flux Synthesis, in Proceedings of Conference on Effective Use of Computers in the Nuclear Industry, CONF-690401 (1969) 271.
6. C.H. Adams and W.M. Stacey, Jr., Nuc. Sci. Eng. 54, 20 (1974).
7. J.B. Yasinsky and S. Kaplan, "Synthesis of Three Dimensional Flux Shapes Using Discontinuous Sets of Trial Functions", Nuc. Sci. Eng. 25, 426 (1967).
8. R.J. Pryor and W.E. Graves, "Response Matrix Method for Treating Reactor Calculations", p. VII-179, "Mathematical Models and Computational Techniques for Analysis of Nuclear Systems". CONF 730414-P2, Ann Arbor, Mich. 1973.
9. Z. Weiss and S. Lindahl, "High Order Response Matrix Equations in Two-Dimensional Geometry", NSE 59, 168 (1975).
10. J.G. Kollas and A.F. Henry, "The Determination of Homogenized Group Diffusion Theory Parameters", Nuc. Sci. Eng. 60, 464 (1976).
11. B.A. Worley and A.F. Henry, "Spatial Homogenization of Diffusion Theory Parameters", MIT Report MITNE-210 (September 1977).
12. A. Kavensky, "Neptune: A Modular Scheme for the Calculation of Light Water Reactors", Proc. Conf. on Computational Methods in Nuclear Engineering, CONF-750413, p. V-27, Charleston, S.C. (1975).
13. D.A. Botelho, "Multidimensional Finite Element Code", Ph.D. Thesis, MIT Department of Nuclear Engineering (1976).
14. D.L. Delp, et al., "Flare, A Three Dimensional Boiling Water Reactor Simulation", GEAP-4598, General Electric Co. (1964).
15. L. Goldstein, F. Nakache and A. Varas, "Calculation of Fuel Cycle Burning and Power Distribution of Dresden-1 Reactor with the Trilux Fuel Management Program", Trans. Amer. Nuc. Soc. 10, 300 (1967).
16. S. Langenbuch, W. Maurer and W. Werner, "Simulation of Transients with Space-Dependent Feedback by Coarse Mesh Flux Expansion Method", CSNI/NEACRP Specialists' Meeting on New Developments in Three-Dimensional Neutron Kinetics and Review of Kinetics Benchmark Calculations, Garching (Munich), Jan. 22-24, 1975.
17. H. Finnemann and M.R. Wagner, "A New Computational Technique for the Solution of Multidimensional Neutron Diffusion Problems", presented at the International Meeting of Specialists on "Methods of Neutron Transport Theory in Reactor Calculations" Bologna, Italy (Nov. 1975).
18. R.A. Shober, R.N. Sims, A.F. Henry, Nucl. Sci. Eng. 64, (October 1977).
19. H. Finnemann and M.R. Wagner, "A New Computational Technique for the Solution of Multidimensional Neutron Diffusion Problems", International Meetinf of Specialists on "Methods of Neutron Transport Theory in Reactor Calculations", Bologna, Italy, November 3-5, 1975.

20. A.V. Vota, N.J. Curlee and A.F. Henry, WIGL-3 -- A Program for the Steady-State and Transient Solution of the One-Dimensional, Two-Group, Space-Time Diffusion Equations Accounting for Temperature, Xenon and Control Feedback, Bettis Atomic Power Laboratory Report WAPD-TM-788 (1969).

21. J.B. Yasinsky, M. Natelson and L.A. Hageman, TWIGL -- A Program to Solve the Two-Dimensional, Two-Group, Space-Time Neutron Diffusion Equations with Temperature Feedback, Bettis Atomic Power Laboratory Report WAPD-TM-743 (1968).

22. J.W. Stewart and M.R. Buckner, Trans. Amer. Nuc. Soc. 17, 255 (1973).

23. D.R. Ferguson and K.F. Hansen, "Solutions of the Space Dependent Reactor Kinetics Equations in Three Dimensions", Nuc. Sci. Eng. 51, 189 (1973).

24. W. Werner, "Mathematical Methods Applicable to Space Time Kinetics", Proc. of Specialists Meeting on Reactivity Effects in Large Power Reactors, Ispra, October 1970.

25. R.J. Pryor, "Recent Developments in the Response Matrix Method", Proc. of Conf. on Advanced Reactors: Physics, Design and Economics, Atlanta, Georgia, September 1974 (p. 169).

26. C.D.D. deAlmeida and A.F. Henry, "Use of Response Matrix Techniques in Nuclear Reactor Kinetics", MIT Report MITNE-177 (October 1975).

27. Michael Todosow, "The Application of Finite Element Methods to Reactor Kinetics Problems", MIT Doctoral Thesis, Department of Nuclear Engineering (1977).

28. L.N. Ussachoff, "Equations for Importance of Neutrons, Reactor Kinetics and Perturbation Theory", Proc. International Conference on the Peaceful Uses of Atomic Energy, Vol. 5, pp. 503-570 (1955).

29. K.O. Ott and D.A. Meneley, "Accuracy of the Quasistatic Treatment of Spatial Reactor Kinetics", NSE: 36, 402-411 (1969).